Department of applied mechanics

Development of methods for modelling the failure of quasi-brittle materials

Juha Kuutti

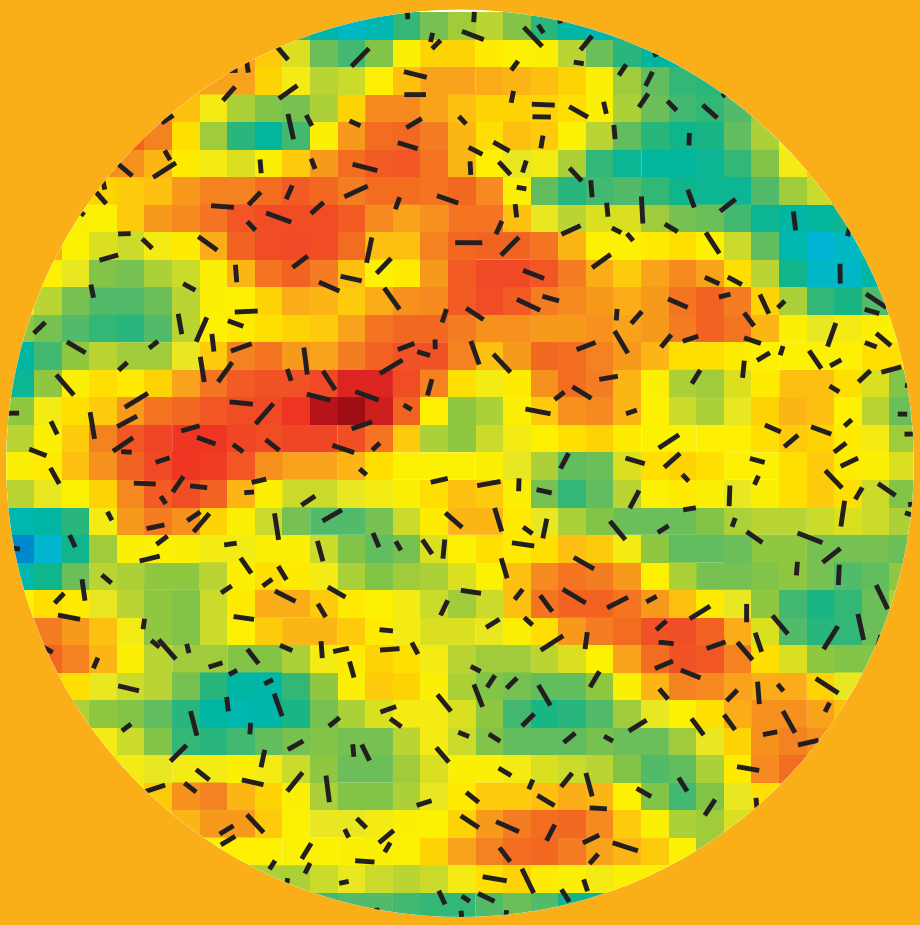

Aalto University

DOCTORAL DISSERTATIONS

Aalto University publication series
DOCTORAL DISSERTATIONS 192/2020

Development of methods for modelling the failure of quasi-brittle materials

Juha Kuutti

A doctoral dissertation completed for the degree of Doctor of Science (Technology) to be defended, with the permission of the Aalto University School of Engineering, on 15 December 2020 at 13:00. Remote connection link: https://aalto.zoom.us/j/64875493481

Aalto University
School of Engineering
Department of applied mechanics
Mechanics of Materials

Supervising professor
Professor Arttu Polojärvi, Department of Mechanical Engineering, Aalto University, Finland

Thesis advisor
Dr. (Tech.) Kari Kolari, VTT Technical Research Centre of Finland, Finland

Preliminary examiners
Professor Mahmoud Mousavi, Department of Materials Science and Engineering, Division of Applied Mechanics, Uppsala University, Sweden

Professor Rocky Taylor, Faculty of Engineering and Applied Science, Memorial University, Canada

Opponent
Professor Rocky Taylor, Faculty of Engineering and Applied Science, Memorial University, Canada

Aalto University publication series
DOCTORAL DISSERTATIONS 192/2020

ISBN 978-952-64-0147-8 (printed)
ISBN 978-952-64-0148-5 (pdf)
ISSN 1799-4934 (printed)
ISSN 1799-4942 (pdf)
http://urn.fi/URN:ISBN:978-952-64-0148-5

Unigrafia Oy
Helsinki 2020

Finland

Printed matter
4041-0619

Aalto University

Abstract

Aalto University, P.O. Box 11000, FI-00076 Aalto www.aalto.fi

Author
Juha Kuutti

Name of the doctoral dissertation
Development of methods for modelling the failure of quasi-brittle materials

Publisher School of Engineering

Unit Department of applied mechanics

Series Aalto University publication series DOCTORAL DISSERTATIONS 192/2020

Field of research Mechanics of Materials

Manuscript submitted 4 November 2020 **Date of the defence** 15 December 2020

Permission for public defence granted (date) 5 November 2020 **Language** English

☐ **Monograph** ☒ **Article dissertation** ☐ **Essay dissertation**

Abstract

The fracture and failure of quasi-brittle materials such as concrete and rock is a complicated process and difficult to model numerically. Such materials are heterogeneous and contain small internal defects and often fail in a quasi-brittle manner, caused by the growth and coalescence of the internal cracks, which adjoin to cause a macroscopic fracture with a considerable fracture process zone. The aim of this work is to develop methods for modelling the different phases of the failure process of quasi-brittle materials, starting from the behaviour of microcracks, onto the coalescence of the microcracks into macrocracking and finally to the continuous propagation of the macrocracks. The methods are based on fracture mechanics, continuum mechanics and numerical techniques and they were developed to be compatible with commercial finite element software.

A combined analytical-numerical method for capturing the effects of microcracks on a continuum scale is presented and applied for large arrays of microcracks. The results show that the interaction of the microcracks is essential as it increases the susceptibility to fracture and affects the material's continuum response.

Crack interaction plays a key role in compressive failure, which is demonstrated by studying wing-crack growth under compression. The growth of wing-cracks can lead to compressive failure, but the growth is easily halted by lateral confinement. The numerical study of 3-D wing-crack systems suggests that the interaction of suitably oriented crack systems can overcome the arresting effects of lateral confinement, leading to compressive failure.

A remeshing method was developed to discretize internal fracturing, based on a fictitious crack approach. Directional softening of the material creates a stress-free plane, which can be converted into a free surface without disturbing the equilibrium. The method was implemented on top of Abaqus FE software and demonstrated with simple test cases.

The post-failure phase of the failure process was captured with a cohesive surface method implemented in Abaqus. Cohesive elements that are potential fracture locations were inserted at each element boundary and the fragmentation continuously progresses as the interface elements fail. The crushing of an ice sheet simulated with the method predicted failure modes, contact forces and high-pressure locations similar to that observed experimentally.

The development of quasi-brittle failure modelling methods is gaining new momentum with the increase of computational power, which allows the application of more sophisticated tools. This work contributes to that field with new methods, case studies and novel results relevant for the engineering community.

Keywords quasi-brittle materials, failure and fracture, numerical modelling, finite element method, fracture mechanics, cohesive zone models, discrete cracking

ISBN (printed) 978-952-64-0147-8 **ISBN (pdf)** 978-952-64-0148-5

ISSN (printed) 1799-4934 **ISSN (pdf)** 1799-4942

Location of publisher Helsinki **Location of printing** Helsinki **Year** 2020

Pages 160 **urn** http://urn.fi/URN:ISBN:978-952-64-0148-5

Tekijä
Juha Kuutti

Väitöskirjan nimi
Kvasihauraiden materiaalien murtumisen mallinnusmenetelmien kehitys

Julkaisija Insinööritieteiden korkeakoulu

Yksikkö Sovelletun mekaniikan laitos

Sarja Aalto University publication series DOCTORAL DISSERTATIONS 192/2020

Tutkimusala Lujuusoppi

Käsikirjoituksen pvm 04.11.2020 **Väitöspäivä** 15.12.2020

Väittelyluvan myöntämispäivä 05.11.2020 **Kieli** Englanti

☐ **Monografia** ☒ **Artikkeliväitöskirja** ☐ **Esseeväitöskirja**

Tiivistelmä

Kvasihauraan materiaalin murtumisprosessi on monimutkainen ja vaikea mallintaa. Tällaiset materiaalit ovat heterogeenisia ja sisältävät sisäisiä vikoja, jotka kuormituksen alla kasvavat ja yhdistyvät makrosäröksi, jonka kärjessä on merkittävä prosessivyöhyke. Tämän työn tavoitteena on kehittää menetelmiä mallintamaan kvasihauraiden materiaalien murtumisprosessin eri vaiheita alkaen mikrosäröjen käyttäytymisestä ja niiden yhdistymisestä makrosäröiksi ja päättyen makrosäröjen etenemiseen sekä materiaalin jatkuvan murtumisen kuvaamiseen. Kehitetyt menetelmät pohjautuvat murtumismekaniikkaan, kontinuumimekaniikkaan sekä numeerisiin tekniikoihin ja ne suunniteltiin yhteensopiviksi elementtimenetelmään ohjelmistojen kanssa.

Työ esittää analyyttisen-numeerisen menetelmän, joka kehitettiin kuvaamaan mikrosäröjen vaikutuksia materiaalissa. Menetelmällä mallinnettiin tapauksia, joissa materiaalissa on suuri joukko pieniä alkusäröjä. Tulosten perusteella säröjen vuorovaikutus on tärkeä huomioida, koska se lisää materiaalin alttiutta murtumiselle ja vaikuttaa materiaalin kontinuumikäyttäytymiseen.

Säröjen vuorovaikutus on tärkeässä roolissa myös materiaalin puristusmurrossa, mikä demonstroitiin mallintamalla siipisäröjen (wing crack) yhdistymisen aiheuttamaa puristusmurtoa. Työssä esitetty 3-D siipisärösysteemeiden mallinnus osoittaa, että säröjen vuorovaikutuksen särönkasvua edistävä vaikutus voi ylittää lateraalisen puristuksen särönkasvua pysäyttävän vaikutuksen, mikä voi mahdollistaa puristusmurron myös

Työssä esitetään menetelmä laskentamallin uudelleenverkotukseen, joka muuttaa materiaalimallin ennustamat sisäiset säröt diskreeteiksi. Materiaalin suuntautunut pehmeneminen johtaa sisäiseen jännityksettömään tasoon, joka voidaan muuttaa vapaiksi pinnoiksi häiritsemättä ratkaisun tasapainoa. Menetelmä on yhteensopiva Abaqus –elementtimenetelmäohjelmiston kanssa ja sen toimivuus demonstroitiin yksinkertaisilla testitapauksilla.

Jatkuvan murtumisen vaihe kuvattiin työssä käyttäen koheesiivisiin elementteihin pohjautuvaa mallinnustekniikkaa, joka implementoitiin Abaqus –elementtimenetelmäohjelmistoon. Materiaalin säröily keskittyy kontinuumielementtien rajapinnoissa oleviin koheesiivisiin elementteihin, joiden vaurioituminen mahdollistaa elementtien irtoamisen toisistaan ja siten materiaalin fragmentoitumisen. Menetelmää sovellettiin kuvaamaan jäälevyn murtumista puristuksessa. Simulaation ennustamat vauriomuodot, kontaktialueet ja –voimat olivat samankaltaisia referenssikokeiden kanssa.

Tietokonekapasiteetin kasvu edistää tutkimusta kvasihauraiden materiaalien mallinnuksesta ja mahdollistaa kehittyneempien menetelmien käyttöönoton. Tämä työ on edistänyt tätä tutkimusalaa kehittämällä uusia menetelmiä ja soveltamalla niitä relevantteihin tarkastelutapauksiin sekä uusilla tuloksilla, jotka ovat merkityksellisiä insinööriyhteisölle.

Avainsanat kvasihauraat materiaalit, murtuminen, numeerinen mallinnus, element-timenetelmä, murtumismekaniikka, koheesiomallit, diskreetti murtuma

ISBN (painettu) 978-952-64-0147-8 **ISBN (pdf)** 978-952-64-0148-5

ISSN (painettu) 1799-4934 **ISSN (pdf)** 1799-4942

Julkaisupaikka Helsinki **Painopaikka** Helsinki **Vuosi** 2020

Sivumäärä 160 **urn** http://urn.fi/URN:ISBN:978-952-64-0148-5

Preface

This work has been long in the making. The first steps towards this thesis were taken already in 2008-2009 when there was active jointly and industry-funded research of ice-structure interaction, which resulted in the first two publications of this work. After that, there were longer pauses as my research focused more on the strength and fracture mechanical aspects topical for the nuclear industry in Finland. Again in 2016, the Academy of Finland funded project to study discrete failures in ice restarted my postgraduate studies, resulting in the third paper of this thesis. The publication of the third paper gave new motivation to complete the studies and I then started the preparation of the final part of the work. Working from home because of Covid-19, this thesis was prepared at the same time as the fourth publication was being finalized.

I would not have gotten here if it was not for PhD Kari Kolari, his guidance and the countless discussions we have had about the mechanics of brittle failure and how to capture it numerically. Kari has co-authored all of the papers included in the thesis and deserves my biggest thank you for making it possible for me to complete this project. I wish to thank my other coworkers at the VTT Technical Research Centre of Finland for their support and fruitful ideas, particularly my manager Lic. Tech. Arja Saarenheimo for allowing me to seek projects, which allowed me to pursue this research. I express my gratitude also to the people at Aalto University, namely professors Arttu Polojärvi and Iikka Virkkunen, who have pushed me forward and increased my understanding of solid and fracture mechanics.

Finally, I thank my loved family for allowing me to spend any free time I had writing this. Kaisa and Jussi, never stop learning new things.

Helsinki, 8 November 2020
Juha Kuutti

Contents

List of Publications

This doctoral dissertation consists of a summary and of the following publications, which are referred to in the text by their Roman numerals.

I. Numerical assessment of the effects of microcrack interaction in AM components. Kuutti, J. & Kolari, K., 2020, In: Computational materials science. 184. 12 p.

II. Interaction of periodic arrays of wing cracks. Kuutti, J. & Kolari, K., 2018, In: Engineering Fracture Mechanics. 200, p. 17-30, 14 p.

III. A local remeshing procedure to simulate crack propagation in quasi-brittle materials. Kuutti, J. & Kolari, K., 2012, In: Engineering Computations. 29, 2, p. 125-143, 19 p.

IV. Simulation of ice crushing experiments with cohesive surface methodology. Kuutti, J., Kolari, K. & Marjavaara, P., 2013, In: Cold Regions Science and Technology. 92, p. 17-28, 12 p.

Author's Contribution

Publication I: Numerical assessment of the effects of microcrack interaction in AM components.

The author was the primary author of the publication and prepared the manuscript. The author developed the crack interaction code, its integration with Abaqus and other subroutines used in the work. The author also performed the modelling and simulations presented in the paper and analysed the results. Kari Kolari contributed to the research with expertise on microcrack modelling and their continuum homogenization.

Publication II: Interaction of periodic arrays of wing cracks.

The author was the primary author of the publication and prepared the manuscript. The author developed the Matlab-code to evaluate the interaction of the cracks and performed the calculations using the code and analysed the results. Kari Kolari contributed to the paper with expertise and suggestions of how to mathematically model the wing cracks and how to interpret the obtained results.

Publication III: A local remeshing procedure to simulate crack propagation in quasi-brittle materials.

The author was the primary author of the publication and prepared the manuscript. The author developed the remeshing method, wrote the material model subroutines and mesh update codes, performed the modelling and simulations and interpreted the results. Kari Kolari contributed to the research by helping to develop the material model and participated in the development of the numerical remeshing approach.

Publication IV: Simulation of ice crushing experiments with cohesive surface methodology.

The author was the primary author of the publication and prepared the manuscript. The author implemented the modelling technique, wrote the material model subroutines and element erosion routines and performed the modelling and simulations and interpreted the results. Kari Kolari contributed to the research by helping to develop the cohesive model for ice, provided expertise on the physical failure process of ice and participated in the result analysis. Pieti Marjavaara was responsible for performing the experiments and provided the test results used for comparison.

Original features

The following features are believed to be original.

1. Numerical assessment of the effects of microcrack interaction in AM components

A novel approach to capture the interaction of internal and surface cracks, sensitive to the mutual locations of the cracks, within a continuum finite element framework was developed and implemented in the commercial FE code Abaqus. The method was applied to provide new results on the macroscale response of additive manufactured components containing a large number of manufacturing flaws.

2. Interaction of periodic arrays of wing cracks

A novel approach for modelling wing crack interaction in 3-D was developed by combining existing methods that describe crack interaction and wing crack behaviour. As a new result, the interaction and subsequent macroscale failure of quasi-brittle materials due to growth and coalescence of wing cracks was shown to be possible also in a 3-D setting.

3. A local remeshing procedure to simulate crack propagation in quasi-brittle materials

The developed method to introduce explicit cracking into a finite element mesh based on an anisotropic continuum damage model was first of its kind, particularly for its capability to model dynamic quasi-brittle failure in 3-D geometries. The method, validated with results of simple experiments from the literature, had subsequent use in describing the continuous large-scale failure process of a quasi-brittle material.

4. Simulation of ice crushing experiments with cohesive surface methodology

The adopted approach for modelling the quasi-brittle failure process was implemented within the commercial FE code Abaqus because such an implementation was not available previously. As a completely novel application, the method was used to simulate the continuous local failure process of ice. The performed case study provided a validation to the approach. It was shown that the approach can predict the progress of the continuous ice crushing process both qualitatively and quantitatively.

1. Introduction

1.1 Background

The topic of this work is the numerical modelling of the failure of quasi-brittle materials. The failure of brittle materials, such as glass, is caused by an instantaneous fracture with little permanent deformation and dissipation of energy, as opposed to a ductile failure or plastic collapse where significant plastic deformation occurs. The term quasi-brittle is used to denote the fact that the material, under stress levels leading to its failure, does not fail instantly but experiences some subcritical damage and energy dissipation but negligible plastic strains before the ultimate failure (Bažant and Planas, 1998; Lemaitre and Desmorat, 2005). A distinctive feature in a quasi-brittle material with a macroscopic crack is the existence of a fracture process zone which is large compared to the cross-section dimensions (Bažant, 2004). The difference between the material and failure types can be visualized with the fracture process zones ahead of a macroscopic crack, as shown in Figure 1.

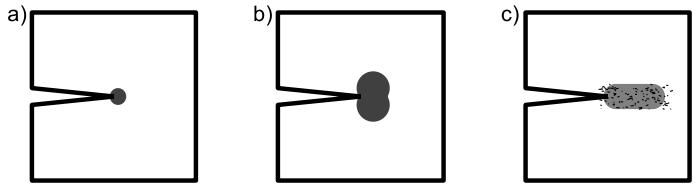

Figure 1. Fracture process zones in brittle materials (a: stress singularity at the crack tip), ductile materials (b: plastic zone at the crack tip) and quasi-brittle materials (c: microcracking and a large fracture process zone at the crack tip).

Natural materials such as concrete, rock and ice are heterogeneous and contain pores, inclusions, mismatching grain boundaries and other discontinuities that serve as nucleation sites for internal cracks. Under certain conditions, such materials often fail in a brittle or quasi-brittle manner, caused by the growth and coalescence of a large number of small distributed cracks, adjoining to cause a macroscopic fracture with a fracture process zone (Bažant and Planas, 1998). Favourable conditions to ensure brittle or quasi-brittle behaviour are specific to each material, but typically require low temperature, a fast loading rate and a moderate confinement pressure. The focus of this work and the applicability of the presented models are limited to this regime.

The understanding and accurate prediction of the failure behaviour of quasi-brittle materials is essential in many engineering applications. For example, a quantitative prediction of how concrete fractures is essential in designing resilient structures and buildings, while the modelling of the faulting of rock is an essential aspect in geotechnical engineering and rock crushing. In the arctic region, the failure of ice governs the ice-induced loads on icebreakers and offshore structures.

Numerical modelling tools are often required to represent the failure process on a scale relevant to the structure or process under consideration. The challenges in modelling the fracture behaviour of quasi-brittle materials arise from the inherent heterogeneity of the materials, the difficulties in capturing the microscale damaging behaviour that leads to macroscale cracking, and the specific characteristics of different quasi-brittle materials. Moreover, the traditional continuum-based simulation tools, such as the finite element method, have traditionally focused on the prediction of the first failure event and the response of static, predefined cracks in the material. It is cumbersome to model the typical features of the quasi-brittle failure process, from the initiation and propagation of microcracking to the subsequent macrocracking and the post-failure fragmentation of the material, because neither the fracture pattern nor its evolution are typically known *a priori*.

Concrete and rock have been used as building materials long before the development of fracture mechanical or numerical methods to describe the failure behaviour of the materials. Particularly for concrete, the consideration of the internal fracturing and resulting macrocracking has provided significant insights into the assessment of structural load-bearing capacity over the traditional elastic-plastic continuum-based design approaches (Bažant and Planas, 1998). Shortly after the pioneering works in fracture mechanics by Irwin (a good review of the history of fracture mechanics is given by Anderson (2017)), fracture mechanics and crack considerations were first applied to concrete in the 1960s, but with limited success (Bažant and Planas, 1998; Kumar and Barai, 2011). The discrepancy between classical fracture mechanics and failure of concrete was later found to be caused by the natural length scale of the concrete fracture processes that well exceed the length scale of metal fracturing (Bažant, 2005). Since this discovery, different models have been proposed to take into account the fracture process zone in front of the crack. A notable step forward was taken in the 1970s as Hillerborg and co-workers (Hillerborg, 1991; Hillerborg et al., 1976) proposed a fictitious crack model, which was able to predict the cracking of concrete without assuming a pre-existing crack. This model provided the link between the continuum strength-based and the discrete fracture-based behaviour by assuming the existence of a fracture process zone, inside which the material is softened by microcracking.

The first attempt to incorporate quasi-brittle fracture with finite element calculations was to fully soften the elements that reached tensile strength, either instantaneously (Rashid, 1968) or as a function of strain (Bažant and Oh, 1983). Numerical issues were discovered (Bažant, 1991) and the formulation was ad-

justed towards the fictitious crack model. Developing at the same time as fracture mechanics, continuum damage mechanics has found great use in predicting the softening and failure of quasi-brittle materials (Lemaitre, 1992). The early attempts to represent the quasi-brittle damage discretely were already done using the finite element method (Rashid, 1968), and this method has remained popular to this day, but numerical tools to simulate the fracture process have been continuously improving since. This thesis contributes to this field by introducing and further developing numerical methods for modelling the different phases of the quasi-brittle failure.

Phases of the quasi-brittle failure process

In this work, the numerical modelling of the failure process of quasi-brittle materials is divided into the following four distinct phases:

1. The behaviour of the individual microcracks and the damaging effects of the microcracks on the continuum scale.
2. The propagation, interaction and coalescence of the microcracks during the formation of a macroscopic crack.
3. The forming of the first macroscopic fracture as a discrete feature in the material.
4. The propagation of discrete fractures and the post-failure behaviour of the material.

The different phases are visualized in Figure 2. The contents of this work are divided such that each of these phases is addressed separately.

1.2 Scope and objectives

Consistent with the four phases of the numerical representation of the quasi-brittle failure process shown in Figure 2, four specific aims were set for this work:

1. To develop and apply a method to model the microcrack opening, closing and interaction within a continuum as well as the effects of the microcracks on the macroscopic stiffness and onset of failure.
2. To develop and apply a method to capture the propagation and coalescence of microcracks able to predict the initiation of the first macroscale failure.
3. To develop and apply a method for transferring the predicted macroscale failure, internal to the material, into an explicit crack within a numerical framework.
4. To develop and apply a method suitable for capturing the continuous propagation of the failure process.

The motivation for the work was to develop and take into use easy-to-apply methods that would be suited for solving engineering problems dependent on the accurate representation of the failure process of quasi-brittle materials from the perspective of fracture mechanics, continuum mechanics and numerical methods. Existing techniques that could be applied in modelling the quasi-brittle failure behaviour of structures and components with finite geometries were

not available off-the-shelf when starting this research in the early 2010s and the situation has not considerably improved since. When developing the methods, it was considered important that they were compatible and possible to implement within the pre-existing computational framework, namely commercial finite element software, so that they can be rapidly applied in various calculation cases while taking full advantage of the other capabilities provided by the software.

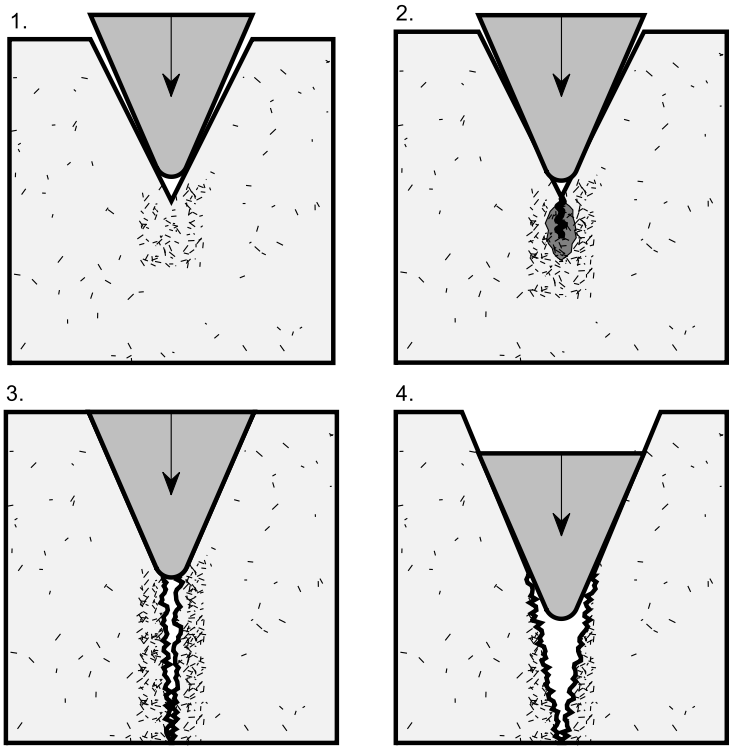

Figure 2. Four phases of the numerical quasi-brittle failure process depicted with crack initiation and growth from a notch loaded by a wedge: 1. Growth and coalescence of microcracks in the high-stressed region; 2. Formation of the first macrocrack and its fracture process zone; 3. Discrete propagation of the macrocrack to split the specimen; 4. Post-failure phase where the wedge is in contact with the crack faces.

The scope of this work is to develop methods and models to capture different aspects of the brittle and quasi-brittle failure behaviour of materials such as concrete, rock and ice. Chapter 2.1 presents how the quasi-brittle failure process is the result of microcrack initiation, growth and coalescence in the material. The focus of the work is on this behaviour and the resulting macroscopic fracturing, which limits the applicability of the models to the conditions where the materials fail as brittle or quasi-brittle in tension, shear or compression with low and

moderate confinement. All ductile processes are outside of the scope of the work, as they include different physical degradation mechanisms.

1.3 Contents of the thesis

This thesis is structured first to present the quasi-brittle failure process from the point of view of the material in Chapter 2.1. This is followed by an overview of the commonly applied numerical tools for modelling quasi-brittle failure in Chapter 2.2. The techniques developed and applied in the publications included in the thesis are described in Chapter 3. Chapter 3.1 describes the mathematical tools to model the internal cracking and Chapter 3.2 describes the approach used to calculate the growth, coalescence of the microcracks and predict the first macroscopic failure. Chapter 3.3 describes the developed method to represent the fracture explicitly in the simulations and Chapter 3.4 presents the applied technique to model the propagation of discrete cracking and post-failure behaviour of the material. The example applications and the cases studied that utilize the developed methods are presented in Chapter 4. The main conclusions of the thesis are given in Chapter 5.

2. Quasi-brittle failure and its modelling

2.1 Quasi-brittle failure process

A brief description of the quasi-brittle failure process is first presented to provide a background to the developments presented later in this work. A distinction has to be made between the quasi-brittle failure behaviour of concrete and rock and the brittle cleavage fracture occurring in glass, ceramics and even ferritic steels at low temperatures. A quasi-brittle fracture is also different from a ductile fracture, where considerable plastic deformation occurs at the crack tip. The characteristic factors are that a quasi-brittle failure is caused by a fracture and there is a fracture process zone of distributed cracking at the crack tip. Such behaviour requires that the loading rate is high enough and the temperature is low enough to suppress any creep deformation or relaxation and the confinement pressure is not sufficient to halt the propagation of the internal cracks. As plastic deformation, i.e. the instantaneous movement of dislocations, is typically insignificant under the considered conditions, the remaining significant deformation mechanism is due to crack growth.

Materials such as concrete, rock and ice are heterogeneous and contain pores, inclusions, mismatching grain boundaries and other discontinuities or stress risers that serve as nucleation sites for the internal cracks (Atkinson, 1987; Schulson and Duval, 2009; Shah et al., 1995). It is commonly accepted that, under rapid mechanical loads, the failure of a seemingly intact material is due to the growth and coalescence of a large number of initiated or pre-existing distributed cracks (Atkinson, 1987; Bažant and Planas, 1998; Kachanov, 1993; Shah et al., 1995). There is a scattered array of existing microcracks or potential initiation sites for microcracks in the material. Under sufficient loading, the first small cracks join to form a macrocrack, which is much larger in length than the microcracks.

Even if there is a pre-existing macroscopic crack in the material, there exists a fracture process zone consisting of microcracks at the crack tip (Brooks, 2013), as shown schematically in Figure 3. Directly behind the crack tip, the matrix material surrounding the inclusions and microcracks is not yet fully damaged and can exert some crack closing forces in this region via unbroken aggregates or other bonds. Further behind the tip, the matrix is fully broken leaving the crack faces free of traction. Ahead of the crack tip in the fracture process zone, new microcracks are nucleated or activated by the crack tip stress concentration. The formation of the fracture process zone dissipates energy and results in an

initially increasing fracture resistance. After the formation of the zone, the crack grows in a self-similar manner without additional fracture resistance. The high stresses ahead of the crack tip are relaxed by the deformation which manifests as microcracking. The material-specific fracturing length scale, which can be interpreted as the size of the fracture process zone, causes a size-effect in the quasi-brittle fracture process (Bažant, 2004). A material can behave in a brittle manner in a large scale component (e.g. large concrete structures) but in a quasi-brittle manner in smaller components (e.g. concrete beams).

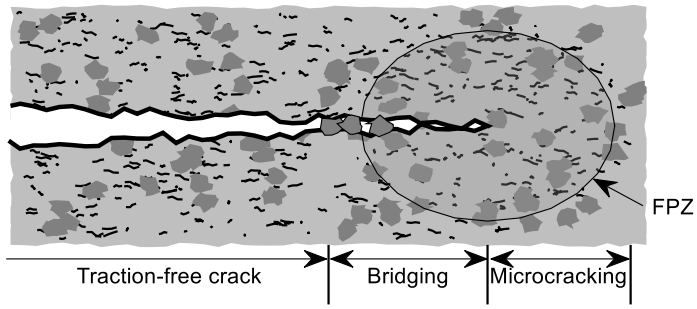

Figure 3. Fracture process zone (FPZ) ahead of a macroscopic crack in a quasi-brittle material. Figure adapted from Anderson (2017).

The failure modes of quasi-brittle materials under different load types are schematically presented in Figure 4. Under tension, quasi-brittle materials demonstrate more brittle-like behaviour as the failure initiates a single macroscopic crack at a critical load level. The tensile fracture is caused a single crack growing in an unstable manner through the material (Figure 4a), driven by the tensile stresses, and does not require an increase of the external load (Bažant and Planas, 1998). This failure mode is typical for rock and ice under tension under brittle conditions and also for concrete in large scale structures (Bažant, 2005).

The strength of quasi-brittle materials is typically much greater in compression than under tension. The compressive failure behaviour of quasi-brittle materials resembles that of brittle materials with initial defects. Under compression, suitably oriented initial cracks extend in a stable manner, requiring an increasing amount of load to propagate. This continues until they coalescence to cause the final failure (Renshaw and Schulson, 2001). Different mechanisms have been proposed to describe how the global compressive stresses can slide and open the internal cracks to enable crack propagation (Lehner and Kachanov, 1996; Wang and Shrive, 1995). A common postulate behind the different models for microcracking is that compressive loading leads to frictional sliding on the pre-existing inclined main cracks, which results in shear deformation at the main crack tips and the formation of small tensile crack extensions at the tips, often denoted as wings (Horii and Nemat-Nasser, 1985), and also along the main crack (Renshaw and Schulson, 2001). As the loading is continued, the cracks tend to turn towards the direction of the maximum external compression

causing a failure mode that appears to split the material parallel to the direction of the applied compression, hence the name axial splitting (Figure 4b). This process has been observed experimentally in planar specimens and see-through materials (Germanovich and Dyskin, 2000; Horii and Nemat-Nasser, 1986; Iliescu and Schulson, 2004).

Under uniaxial compression in the brittle regime, the axially oriented cracks open in the lateral direction, causing a volumetric expansion of the material. The failure mode of brittle and quasi-brittle solids shifts towards a shear-like mechanism if a confining lateral load is applied (Figure 4c). With small confining pressures, the compressive failure tends to be in the axial direction, but increasing the lateral confinement transforms the fault mode into a shear-type failure as the lateral stresses increase internal friction and stop the axial growth of the cracks. Shear failure has been attributed to the cumulative growth of an array of adjacent internal flaws, suitably oriented in a direction that appears as shear faulting in the macroscale (Horii and Nemat-Nasser, 1985). Large confining pressures halt the propagation of the internal cracks leading to ductile failure (Renshaw and Schulson, 2001).

Tensile failure can be considered as a uniaxial phenomenon whereas compressive and shear failures are triaxial in nature. As the deformation is caused by the opening of planar crack-like defects within the material, the response of the material is inherently anisotropic even before the fracture. For example, compressive loads can close the tensile cracks, which recovers much of the stiffness of the material, before the compressive failure process takes place. Figure 4 visualizes the different failure types. The shear failure, in particular, may take a different macroscopic appearance, depending on the amount of confinement and boundary conditions (Bažant and Planas, 1998). For example, a frictional restraint on the loading surfaces alters the failure mode towards a conical shape at both ends of the specimen (Bažant and Xiang, 1997).

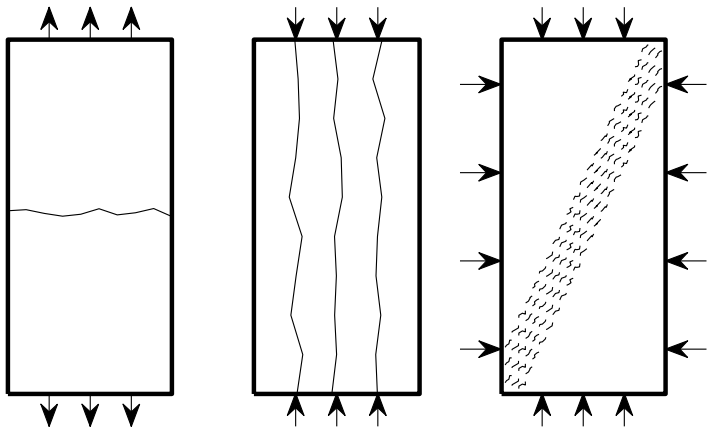

Figure 4. Possible failure modes of a quasi-brittle specimen under a) tension; b) unconfined compression (axial spitting); c) confined compression (shear failure). Adapted from (Bažant and Xiang, 1997).

The failure process outlined above holds true in general for concrete, rock and ice in the brittle and quasi-brittle regime. The brittleness in tension and the existence of a fracture process zone is widely acknowledged for the materials (Bažant and Planas, 1998; Brooks, 2013; Schulson and Duval, 2009) along with the use of the fracture process zone concept (e.g. Dempsey et al. 2018; Elices et al., 2002). The initiator for a brittle-like failure depends on the material type, but once an internal crack reaches a critical state, it propagates through the material without resistance. Subcritical cracking and the formation of the fracture process zone may provide the material some apparent toughness before the final failure in tension (Bažant and Planas, 1998). Models describing compression failure, based on the coalescence of internal flaws have, been applied for concrete, rock and ice (Bažant and Planas, 1998; Renshaw and Schulson, 2001). Such models, based on frictional sliding of the internal cracks, are strongly dependent on the initial defect distributions and the frictional behaviour of the crack surfaces (see Section 3.2) but the kinematics of the failure process remain unchanged.

Ductile deformation and the resulting failure behaviour falls outside the scope of this work. The ductile deformation of rock, ice and concrete is typically caused by creep, which requires sufficiently long loading times, high homologous temperatures and at least moderate confining pressures to halt the propagation of the internal cracks (Bažant and Planas, 1998; Paterson and Wong, 2005; Renshaw and Schulson, 2001). Also the length scale, set by the fracture process zone of a cracked structure, can induce ductile-like behaviour if the structural dimensions are of the same order of magnitude as the crack size (Bažant, 2005). As the temperature or confining pressure decreases or loading rate or structural dimensions increases, the failure behaviour becomes increasingly brittle. The ductile-to-brittle transition point depends on the material, although the transition occurs gradually over a range of values around the transition point (Schulson and Duval, 2009). For concrete, the transition criteria is typically expressed using the structural size (Bažant, 2005). Rock mechanics models typically link brittleness with the confining pressure (Paterson and Wong, 2005) and ice failure models are expressed as a function of strain rate (Schulson and Duval, 2009). Sea and freshwater ice, in particular, are often at a temperature near the melting point and the rate of deformation can be slow and the confining pressure large, for example in a case where an ice sheet is pushed against a structure by wind, rendering the material susceptible for ductile creep deformation.

When simulating the fracture of quasi-brittle materials, the vast number of randomly located cracks means the material needs to be treated as a continuum by averaging the behaviour and effects of the microcracks onto the macroscopic level. The next section outlines techniques from the modelling of the microcracks and macrocracks to the continuum models needed to capture the macroscopic softening and finally the techniques needed to represent the fractures within a numerical framework.

2.2 Modelling of quasi-brittle failure

The basic principles of fracture mechanics are first discussed in Chapter 2.2.1. Fracture mechanics is needed to describe the behaviour of cracks in a material and it also forms the foundations of the physically motivated continuum constitutive models of cracking that are discussed in Chapter 2.2.2. Chapter 2.2.4 concludes the overview by presenting the different approaches needed to bridge the gap between the continuum damage models and discrete cracking.

2.2.1 Fracture mechanics

Fracture mechanics is a theory for describing the behaviour and effects of crack-like flaws in materials. In this work, fracture mechanics, and linear fracture mechanics in particular, is applied to describe the initial response and early growth of the microcracks in a quasi-brittle material. This allows the behaviour of the individual microcracks and the macroscopic crack to be predicted, with certain limitations discussed below. A thorough presentation of the fundamentals of fracture mechanics is given by Anderson (2017).

Linear elastic fracture mechanics (LEFM) deals with sharp notches in elastic materials. In LEFM, the stress concentration at the crack tip is postulated to be singular and strongly attenuating away from the crack tip. The amplitude and exact shape of the stress field depends on the boundary conditions for the crack, but it always contains a singularity at the crack tip. The strength of the singularity is represented by the stress intensity factor (SIF) parameter, which is a single-parameter description of the stress intensity at the crack tip and depends on the crack size, applied loading and component geometry. Since it can be considered to be the most important parameter in linear fracture mechanics, SIF solutions have been developed and documented for numerous crack shapes and component geometries (Murakami, 1992; Tada et al., 2000). The SIF is a characterizing parameter for the onset of failure in brittle materials (Bažant and Planas, 1998). The critical value of the stress intensity factor is a material property denoted as the fracture toughness K_c. Typically, failure is assumed to occur when the SIF reaches the value of K_c.

The deformation of a crack can be divided between three separate modes. Mode I consists of opening normal to the crack plane, Mode II consists of in-plane shear deformation, parallel to the crack extension direction, while Mode III is defined by the crack face out-of-plane shear movement, perpendicular to the crack front. Figure 5 shows a visual representation of the modes. In the linear regime, each of the modes induces a stress field which is proportional to the magnitude of the crack loading or crack displacement.

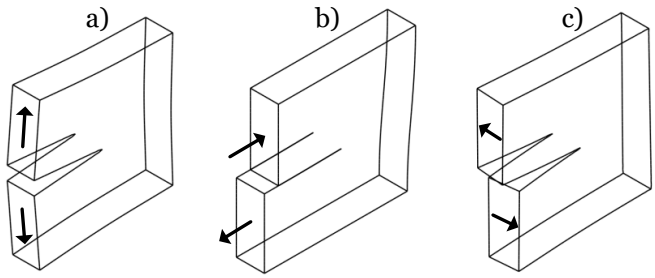

Figure 5. Crack opening shapes in Mode I (a), Mode II (b) and Mode III (c). The figures show the exaggerated deformation of finite element simulations of a linear elastic body.

In addition to the stress-based parameters, the energy-based concept of energy release rate developed by Irwin (Anderson, 2017, Ch. 2.4) is a useful parameter for describing the fracture behaviour of a crack. It is defined as the available energy to extend the crack by a unit area or unit increment, $G = \frac{d\Pi}{dA}$, and it can also be considered as the change of the potential energy of the body due to the extension of the crack. Considering that the damage is concentrated at the fracture process zone, the change in the potential energy is equal to the amount of energy dissipated at the crack tip due to the crack extension.

The LEFM theory has been developed to address situations where the inelasticity at the crack tip is small. However, the postulate that there are infinite stresses at the crack tip cannot be satisfied in real materials. Instead, there has to be some inelasticity that lowers the stresses to a level which is tolerable by the material. Different models have been developed to capture this crack tip plasticity. Even for quasi-brittle materials, the strip-yield model developed to model the plastic deformation at the crack tip, attributed to Dugdale and Barenblatt (Anderson, 2017, Ch. 2.8.2) is relevant to understanding the similarly formulated cohesive zone models. In the strip yield model visualized in Figure 6, the crack tip is assumed to be located within the plastic zone and crack closure stresses equal to the yield strength of the material are postulated behind the crack tip.

Figure 6. A schematic drawing of the crack tip plastic zone with crack tip opening displacement δ (left) and cohesive stresses of σ_Y at the crack tip (right). Figure adapted from Anderson, (2017).

In the strip yield model, uniform stresses prevail near the crack tip regardless of the crack opening magnitude. The cohesive zone model, also called the fictitious crack model by Hillerborg (1991), is a special case of the strip yield model and is discussed in more detail in the next section. In the cohesive zone models, the closure stresses at the crack tip are not taken as uniform but degrade as a function of crack opening, aiming to capture the partly intact bonds just behind the crack tip and the progression of the failure process (see Figure 3).

LEFM is not applicable as such to describe the fracture of quasi-brittle materials as it applies to cases where the inelasticity at the crack tip is limited to a zone which is small compared to the crack and structural dimensions. As discussed in Chapter 2.1, in quasi-brittle materials there exists a finite size fracture process zone in front of the crack tip due to the microstructural damage in the material. While the LEFM requirements are not satisfied exactly, the concepts of LEFM outlined in this chapter are essential to understanding both the microscale and macroscale crack behaviour modelled in this work. In addition, the LEFM concepts can be applied to capture the behaviour of the microcracks within a material that experiences a predominantly linear response, as applied in Publications I and II included in this work (see Chapters 3.1 and 3.2). Typically, the response of a material containing numerous small internal defects is modelled in an average sense by using different continuum models, some of which are discussed next.

2.2.2 Continuum failure models

This section discusses the continuum modelling of the fracture process of quasi-brittle materials. The discussion starts from the representation of the damaged zone in front of a macroscopic crack and extends to more sophisticated constitutive models aimed in representing the full pre- and post-failure response of the material.

Fracture process zone models

As discussed in Chapter 2.1, a finite region of softened material in front of the macroscopic crack tip, denoted as the fracture process zone (Brooks, 2013), has a central role in the fracture of quasi-brittle materials. The fracture process zone is commonly represented as softening due to microcracking and cohesion over the crack faces with a cohesive zone model, similar to the strip yield model in Figure 6. Figure 7 shows a schematic of the fracture process zone and a cohesive zone model which aims to represent the crack tip inelasticity and the stresses acting in the process zone and in front of the crack tip.

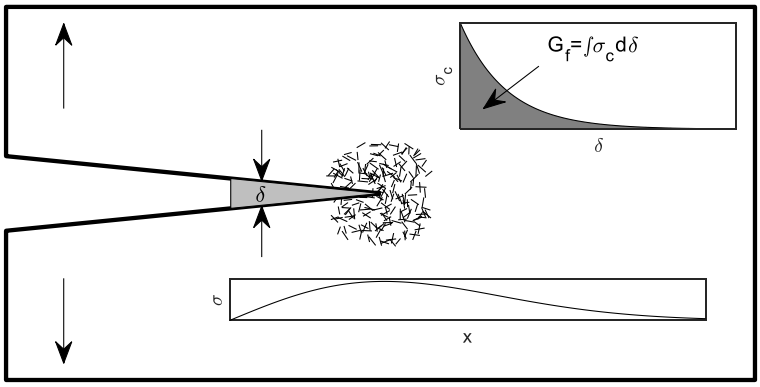

Figure 7. The fracture process zone ahead of a tensile crack and the crack tip stress σ distribution as a function of the distance from the crack tip x. The cohesion stress σ_c is attenuated as a function of the crack tip opening δ. The fracture energy G_f is obtained from the integral of the softening function. Redrawn after Bažant (1986).

Cohesive zone models

In the cohesive zone models, the fracture process zone is typically condensed onto a single line or plane. A well-known example of such models is the Hillerborg's fictitious crack model, which was developed to model concrete fracture (Hillerborg et al., 1976). Unlike the strip yield model, the cohesive zone models assume cohesive stresses which depend on the opening of the crack, as schematically shown in Figure 7. When loading is subjected to a cracked body, the fracture process zone begins to form as the tensile stress at the crack tip reaches the tensile strength. If the loading is continued, the crack propagates while maintaining a stress equal to the tensile strength at the current crack tip. An essential concept in the model is the stress-separation behaviour at the crack tip, which is also related to the fracture energy (Figure 8).

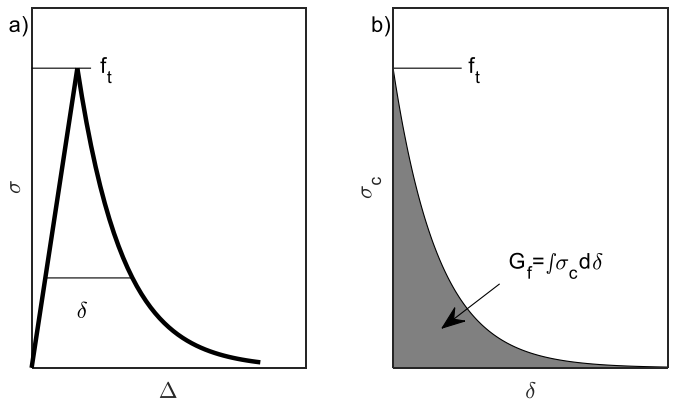

Figure 8. The full uniaxial stress-displacement (σ-Δ) relation obtained with a cohesive zone model (a) and the stress softening relation describing the fracture process (b). The cohesive stress σ_c is attenuated from the tensile strength f_t as a function of the crack tip opening displacement δ.

The stress-separation behaviour is often considered a material property. However, the deviations from the pure Mode I conditions, such as the interaction of the crack with free boundaries or mixed-mode loading conditions, can lead to inconsistencies in the approach (Elices et al., 2002; Planas et al., 2003). The cohesive zone models replace the stress singularity at the crack tip with the description of the fracture process zone while allowing the rest of the material to be treated as elastic. There exist various stress-softening formulations that are intended to capture different physical processes at the crack tip, depending on the material (Anderson, 2017, Ch. 6).

The cohesive zone models assume the existence of a macroscopic crack in the material. In inhomogeneous materials, microcracks, voids and other defects exist even when there are no macroscale cracks. Their combined effect on the continuum response is often denoted as damage (Lemaitre, 1992). Models which are similar to the cohesive zone model can be applied also to capture the tensile failure behaviour of initially macroscopically intact material. As the material is loaded with tension, the microcracks in the material initiate and grow, causing softening. As the tensile strength is reached, the material deteriorates in a local region by forming a macroscopic crack that extends through the specimen. The load required to cause any additional displacement reduces rapidly as shown in Figure 8. Such a behaviour is captured naturally by the cohesive zone model, as demonstrated by Hillerborg (1991). The fracture process is first governed by the macroscopic tensile strength criterion and the failure behaviour of the induced crack is described via the stress softening relation that also yields the amount of energy consumed in the fracture process. Publication IV included in this thesis makes use of the fictitious crack formulation to describe the local softening, fracturing and subsequent crack propagation.

Smeared crack models

Similarly to the cohesive zone models applied in cases without macroscopic cracks, smeared crack models have been developed to capture the softening effects of microcracks in inhomogeneous materials (Bažant and Oh, 1983; Rashid, 1968). Such models assume that the microcracking is uniformly distributed over a finite region, or smeared, in the material (Figure 9), in contrast to the cohesive zone model where the full fracture process zone was condensed onto a single line or plane. The difference between the models is visualized with an elongation profile of a tensile bar in Figure 9.

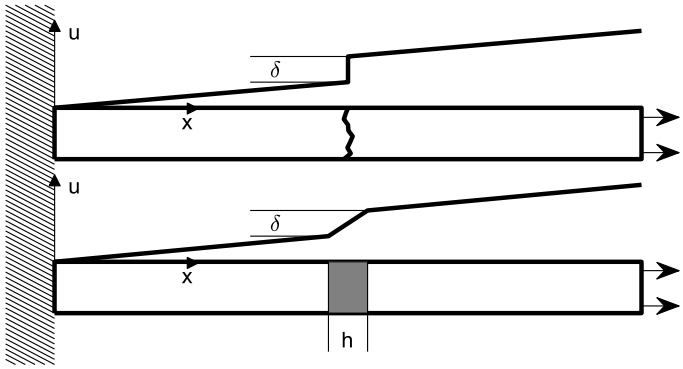

Figure 9. Cohesive crack model (top) and smeared crack model (bottom) failure behaviour of a uniform tensile bar. The elongation profiles (u-x) of both approaches are plotted on top of the bars. The crack opening displacement δ is equal in both models and but it is distributed over a region of width h in the smeared crack model. Figure adapted from Bažant and Planas (1998).

Developed with finite element applications in mind, the smeared crack models describe the onset of fracture as a function of critical stress in a material point and the subsequent softening as a function of applied strain. The approach does not rely on a fracture mechanical description of the fracture process but a predefined continuum description of the effects of the fracturing. While it is easily implementable in the finite element framework, the approach has been found to be numerically unobjective such that different results are obtained with different element sizes (Bažant and Jirásek, 2003). This problem can be alleviated by introducing a length scale into the formulation, similar to the stress vs. crack opening relation in the cohesive zone models. The displacement or energy-based regularization of the softening process forces the global energy dissipation to be mesh-independent (Bažant, 1991), while the different element sizes show different stress-strain behaviours.

Softening and damage concepts

The assumptions concerning the orientation of the microcracking are essential in the smeared crack model as well as in any constitutive model that aims to represent the effects of discrete cracks within a material. The simplest approach is that the microcracking, i.e. damage, is initiated when the tensile strength is reached anywhere in the material. The term damage is attributed to L.M. Kachanov (Chaboche, 1988; Kachanov, 1958), who used the term to denote the density of microcracking of a material undergoing creep deformation. The mathematical formulation of using internal variables to describe damage and its effects on a continuum scale is denoted as continuum damage mechanics (Chaboche, 1988; Lemaitre, 1992). Typically, complete damage manifests as a full or nearly full degradation of stiffness in the loading direction and perpendicular to it. This represents a scenario where one or more cracks have initiated and adjoined on a plane and the material is unable to transmit normal stresses

over this plane or to transmit shear stresses along the plane. Additional assumptions have to be made in the formulation of the response of a cracked specimen in directions oblique to the main loading direction. Different mathematical models have been developed to describe the rotation of the primary cracks and initiation of secondary cracks as the loading direction evolves (Bažant and Planas, 1998). Publication III of this thesis employs a simplified smeared crack formulation to predict the internal softening and damage of quasi-brittle materials.

Geometric interpretation of damage

Mathematically, the cracks and voids in the material are represented via a damage variable, denoted D or ω, that can be a scalar, a vector or a tensor, depending on the formulation. A traditional idealization of the damage is to consider small parallel rods, or springs, that transmit tensile stresses (Figure 10).

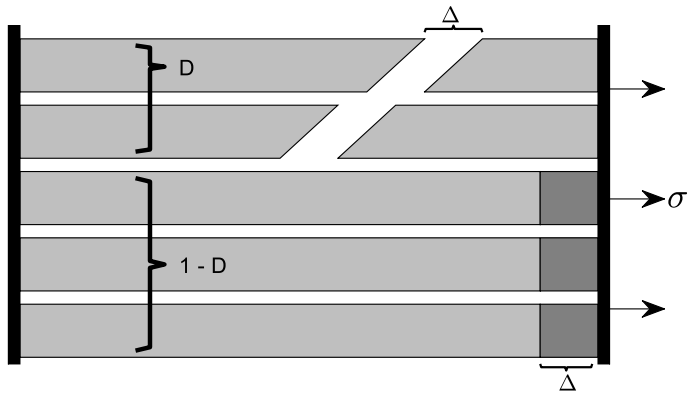

Figure 10. Visual representation of damage with intact and broken tensile bars in a system stretched uniformly with displacement Δ. Figure redrawn after (Bažant and Planas, 1998).

Upon loading to a uniform external strain ϵ, some of the rods fail leaving the others to carry the applied macroscopic stresses σ. The damage parameter represents the area fraction of the damaged rods, $A_{damaged}$, to the total number of rods, A_{total}, (Lemaitre, 1992):

$$D = \frac{A_{damaged}}{A_{total}} \tag{1}$$

Because the springs are parallel, the total stiffness of the system degrades with this ratio and the resulting macroscopic stress due to the uniform strain ϵ is:

$$\sigma = (1 - D)E\epsilon \tag{2}$$

As more springs fail, the macroscopic stress required to obtain the uniform strain ϵ decreases. If the external load is maintained at a constant level (i.e. the macroscopic stress σ is constant), the stresses in the unbroken bars increase due to the damage:

$$\tilde{\sigma} = \frac{\sigma}{1-D} \tag{3}$$

Equation (3) is the definition of the effective stress (Lemaitre, 1992). The average stress fully relaxes as $D \to 1$, while the stress in the last unbroken bars tends to infinity.

The stress-strain relationship of Eq. (2) holds also for the unloading in a stress-softening type model, assuming that there is no permanent deformation caused by the damage. In fact, formulations containing Eq. (2) in different forms are used widely in damage mechanics, often without any specific physical counterpart for the damage variable. In a recent review, Santaoja (2019) discusses different interpretations and candidates for the damage variable based on physical failure mechanisms. For example, the damage parameter of an isotropic elastic solid with spherical microvoids was shown to be well approximated as twice the volume fraction of the voids.

The geometric interpretation of damage, which is the relative amount of cracks and voids in a material, the stiffness degradation and effective stress concepts of damage can be contradictory. Kachanov (1993) demonstrates this with an example of stacked cracks that shield each other. If the cracks are moved closer to each other, the shielding effect between the cracks increases, which also increases the macroscopic stiffness while keeping the geometric interpretation of the damage constant. Kachanov (1993) also argues that the damage variable can also be viewed as the proximity to macroscopic failure. This too can be inconsistent with the geometric interpretation of damage. As more stacked cracks are added to the material, the shielding effects become stronger and the susceptibility to fracture in fact decreases while the relative area of the cracks in the material increases. The shielding effects can play a key role in controlling the growth potential of microcracks in the material as demonstrated in Chapter 3.1.

Constitutive damage models

In the context of this work and the efforts outlined in Chapters 3 and 4, the important result of damage is that it produces a local, directional softening in the material, leading to an oriented macroscale failure. The smeared crack model detailed above is an example of a constitutive damage model, although it is formulated directly as a postulated stress-strain or stress-displacement relationship instead of a more rigorous approach based on the thermodynamic potential of the material (Ottosen and Ristinmaa, 2005). Physically justified potential functions can be constructed assuming e.g. the existence of spherical voids or crack-like defects (Basista and Gross, 1998; Ju, 1991; Nemat-Nasser and Hori, 1993). Although it is preferable to tie the constitutive formulation to the physical response and defects in the material, any form of thermodynamic potential, and the resulting constitutive equations, is allowable if it fulfils the Clausius-Duhem inequality, which mechanically corresponds to a non-negative dissipation of energy (Ottosen and Ristinmaa, 2005).

In the literature, numerous damage models have been proposed to model the fracturing of materials with internal defects. For example, both Ashby and Sammis (1990) and Horii and Nemat-Nasser (1985) have formulated damage models to capture the compression failure of brittle solids based on a fracture mechanical representation of the internal cracks. Both models predict the confined and unconfined compressive strength of brittle materials and associate damage with the magnitude of internal cracking but are not self-standing constitutive

models that would predict the full stress-strain behaviour of the material. Basista and Gross (1998) present a full constitute model using similar crack kinematics to Ashby and Sammis (1990) and Horii and Nemat-Nasser (1985) and based on a complementary energy formulation that results in the complete stress-strain relationships until failure. The formulation associates damage and loss of stiffness with the internal cracks in the material that propagate with increasing loading.

Two popular continuum-based damage models used for quasi-brittle materials are the Barcelona model and the Microplane model. The Barcelona model assumes separate damage variables for tension and compression and is pre-programmed in the Abaqus FE code as a modified version denoted as the Concrete Damaged Plasticity model (Abaqus, 2017; Lee and Fenves, 1998). In the Microplane model, the constitutive behaviour of the material is evaluated simultaneously on several planes with different orientations and the resulting macroscopic constitutive response is a weighted sum over all the microplanes (Bažant et al., 2000). Both models are phenomenological in the sense that they seek to produce the realistic macroscale strength and softening behaviour of quasi-brittle materials without explicit considerations of the cracking at the microscale level in the material.

Regardless of the formulation, the result of the constitutive models is a mathematical representation of the failure. This manifests as the loss of the load-bearing capacity of the material, at least locally. In many engineering applications focused on the prediction of the resistance of the structure, the analysis does not need to capture the post-failure behaviour and knowledge about how the failure propagates in the material is of secondary importance. On the other hand, some failure problems depend fully on the accurate representation of the propagation of failure, such as projectile penetration into concrete targets, the crushing of rocks or the breakage of ice around icebreaking vessels. Numerical modelling of such events requires techniques beyond constitutive models, which are addressed in Chapter 2.2.4. The next chapter outlines how the failure models discussed above have been used to model the brittle and quasi-brittle failure in material-specific applications.

2.2.3 Application of the models for quasi-brittle materials

In simulating the response of concrete, rock and ice, two kinds of material models have remained popular. The first kind is based on the cohesive zone model, in which the crack front or prospective crack line is represented with the cohesive traction-separation law. The second kind relies on a more rigorous continuum-based constitutive modelling approach, suited for the evaluation of damaging anywhere in the material.

Fracture process zone models and cohesive zone models

First, the focus is laid on the application of the cohesive zone models with concrete, rock and ice. The original cohesive zone model by Hillerborg et al. (1976) was developed to model concrete, and the approach has remained popular for concrete fracture ever since. A re-evaluation of the model by Hillerborg (1991)

discusses the generalization of the model for other materials, including rock, through arguments based on the qualitative aspects of the failure process.

A good review of the behaviour of the cohesive zone model is provided by Elices et al. (2002), where the applicability of the model particularly for concrete fracturing but demonstrate how the model applies equally well for acrylic glass when using appropriate parameters is discussed. Emphasis is also placed on the determination of the shape of the softening function. Also Planas et al. (2003) discuss the appropriate shape of the softening function, along with prospective generalizations of the model, such as mixed-mode effects. Bažant (2001) presents a similar evaluation of the common concrete fracture models, with a focus in the cohesive zone model and associated experimental approaches. Bažant, a pioneer in concrete fracture modelling, still publishes works promoting the use of the cohesive zone model to model concrete fracture (Carloni et al., 2019; Hoover and Bažant, 2014).

The cohesive zone model is equally applicable in describing the fracture process zone in rock (Fakhimi and Tarokh, 2013; Hillerborg, 1991). Concrete and rock are often considered together when discussing the applicability of the model for quasi-brittle materials (Bažant and Planas, 1998). A larger-scale practical application of the model for rock fracture is related to hydraulic fracturing (Lecampion et al., 2018). The process is markedly different from traditional fracturing as high-pressure fluid is deliberately injected to the bedrock to assist the fracture. Papanastasiou and Sarris (2017) demonstrate how a pressure-sensitive cohesive zone model is applied to evaluate fracture propagation in bedrock and the crack opening displacement, through which gas and oil are able to flow. A particular requirement in utilising the cohesive zone model for this application is the consideration of the effects of hydraulic pore pressure to the fracture process (Yao et al., 2015).

The models developed to describe the brittle and quasi-brittle failure of concrete and rock are often applied for ice, particularly the cohesive zone model (Dempsey et al., 2018; Mulmule and Dempsey, 1997). The traditional application of the model assumes predefined crack paths, which, in the case of ice brittle fracturing, apply primarily to laboratory or in-situ fracture mechanical specimens loaded in tension. Due to the natural unpredictability of the crack paths, the cohesive model is typically coupled with different numerical techniques developed to capture cracking at near arbitrary locations (see Chapter 2.2.4). A common such application is to define prospective crack locations between all elements in the simulation model. The fracturing of ice has been simulated with this approach using finite elements at least by Gribanov et al. (2018), Gürtner (2009) Lu et al., (2014), and with the discrete element method by Paavilainen et al. (2011) and Polojärvi and Tuhkuri (2013). Publication IV of this work falls into the former category.

Damage mechanics models

Both De Borst (2001) and Bažant (1986) discuss the relationships between the cohesive zone models, focused on single cracks, and the continuum-based models, appropriate for distributed cracking. The softening and fracture process

concepts of the cohesive zone model are often incorporated within damage mechanics models.

As mentioned in Chapter 2.2.2, two of the most popular damage mechanics models, the Barcelona model (Lee and Fenves, 1998), also denoted as the Concrete damaged plasticity model in Abaqus, and the Microplane model (Bažant et al., 2000) have been developed for concrete. The popularity of the models is because of their built-in implementations to commercial finite element software. These damage mechanics models are essentially phenomenological, i.e. aim to produce the correct macroscopic damaging response without detailed considerations of the internal microcracking process. The development of similar models is on-going, to better represent all different phenomena occurring in tension and confined and unconfined compressive failure of concrete within a single model (Červenka and Papanikolaou, 2008; Grassl et al., 2013). The actual mechanics of the fracturing process inside concrete can be captured with extensions of linear elastic fracture mechanics (see Chapter 2.2.1), which is why fracture mechanical models have been incorporated in damage mechanics models such as those developed by Kurumatani et al. (2016) and Mazars and Pijaudier-Cabot (1996).

The actual deformation mechanisms occurring during rock fracturing are largely captured using fracture mechanics, which facilitates the development of mechanistic damage models for rock. The representation of the internal crack kinematics alone, such as those presented by Horii and Nemat-Nasser (1986) and Renshaw and Schulson (2001), do not yield a self-consistent continuum damage mechanics model but need to be coupled with a crack homogenization scheme and a thermodynamical constitutive modelling framework. Such models are applied for rock at least by Basista and Gross (1998), Dragon (2002) and Pensée et al. (2002). New models with the same principles are continuously being developed to take into account new features such as crack interaction (Paliwal and Ramesh, 2008) or fluid pressure, which is essential for modelling hydraulic fracturing (Shojaei et al., 2014).

The mechanics of brittle fracture in ice are similar to those occurring in rock (see Chapter 2.1). Therefore, the models developed for rock fractures can be applied for ice after the recalibration of the parameters and ensuring that the model represents the correct internal fracture mechanisms of ice. Alternatively, the basic principles behind the rock-specific damage mechanics models can be applied to develop novel models for ice fracturing. Kolari (2017) considered the fundamental fracture processes occurring in brittle materials with emphasis on defect patterns representative of ice and formulated a thermodynamically consistent continuum model. The applicability of the model was demonstrated by predicting the failure patterns and macroscopic strength of ice in tension and compression.

More traditional constitutive models, mostly based on plasticity and ductile damage, have been calibrated and applied to model the brittle fracture of ice on a case-by-case basis. For example, von Bock und Polach and Ehlers (2013) used a damage model tied to the evolution of plastic strain to capture the brittle be-

haviour of model ice. Gagnon (2011) utilised the crushable foam model to represent the physical processes observed to occur during the crushing of ice. Derradji-Aouat (2003) proposed a multi-surface failure criterion for ice to reproduce the triaxiality effects and anisotropy observed in the strength values of sea ice. Ince et al. (2017) proposed to use a straightforward stress-strain model based on strength parameters calibrated from experiments. Liu et al. (2011) applied a plasticity-based model to represent the iceberg crushing process during ship-iceberg collisions. Sand (2008) employed plastic models to represent brittle cracking and the subsequent crushing by significantly lowering the strength parameters of the failing elements at the point of failure. Jordaan et al. (1999) and Taylor and Jordaan (2014) utilised a two-term damage mechanics model, which represents both brittle and ductile behaviour simultaneously and aims to capture the phenomena occurring during high-speed compressive failure of ice. Low and high confinement processes were treated separately with separate damage variables. Common to the above models is the fact that they are used to model generally brittle ice in specific ice-structure interaction scenarios, where the ice failure behaviour is more complex than that deducted from uniaxial or triaxial tests. The models specifically fine-tuned for the studied scenario can achieve predictability only in other similar scenarios. Moreover, the discrete nature of the fracturing process requires that the constitutive model need to be supported by a numerical technique able to capture the post-failure phase (see Chapter 2.2.4).

The models mentioned above focused primarily on the brittle and quasi-brittle failure conditions. A large number of models have been developed to capture the ductile failure behaviour of the materials, but it is out of the scope of this work.

2.2.4 Discrete representation of damage

The continuous failure process of quasi-brittle materials is highly complex and may include several different failure mechanisms. An example of a complex fracturing process is the crushing of a concrete slab under the impact from a rigid projectile, as depicted in Figure 11, or the compressive breakage of an ice sheet studied in Publication IV and summarized in Chapter 3.4. Accurate modelling of this kind of a process requires that both the failure behaviour of the material is correctly captured by the constitutive model and the resulting fractures are incorporated in the numerical model as free surfaces that are later able to contact other surfaces of the model. The constitutive models that predict the fracture onset were discussed in the previous chapter and the commonly applied numerical modelling techniques able to capture the discrete fracturing process are the topic of this chapter. The emphasis is on the background of the methods used in the developments presented later in this work. Due to the popularity of the finite element method in structural analysis, most of the approaches to capture discrete cracking are formulated to be compatible with it.

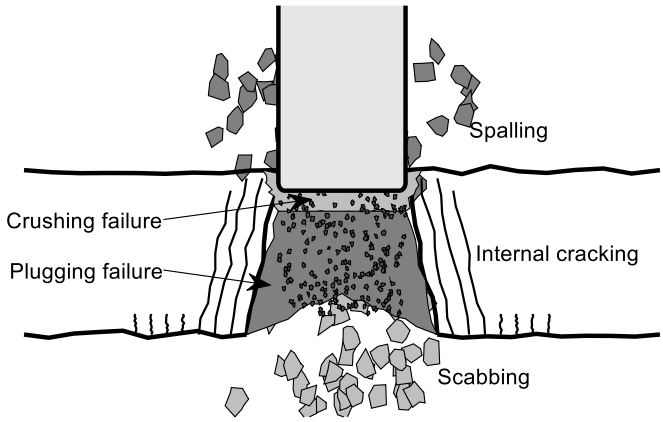

Figure 11. High-speed penetration failure of a concrete slab. Figure adapted from (Q. M. Li et al., 2005).

Traditional finite element method based approaches

The incorporation of linear and elastic-plastic fracture mechanics with finite elements (FE) is well established (Anderson, 2017, Ch. 12) and available in major commercial and open-source FE-codes. The cracks are modelled using the external boundaries of the elements and even specially formulated elements have been developed to model the singularity at the crack tip. Techniques to evaluate the stress intensity factors and energy release rates from a finite region around the crack tip have been developed to avoid the evaluation of the singular terms (Courtin et al., 2005). Publications I, III and IV make use of the finite element method, but not in the sense of traditional fracture mechanics-based modelling of the cracks.

Mesh adaptation techniques

Adding to the approach of representing macroscopic cracks with the free boundaries of the finite element model, crack tip remeshing methods have been proposed to model crack growth, often considering fatigue (e.g. Bremberg and Dhondt, 2009). Maximizing the energy release rate is often used as the criterion for the propagation direction (Anderson, 2017, Ch. 2.11), while the increment of the extension is something limited by the computational capacity. The efforts in Publication III fall within this category but the crack propagation is driven by the smeared crack model. Additionally, commercial implementations of this type, both as a separate codes (e.g. FRANC2D/3D) or third-party add-ons to existing software (e.g. Zencrack, ADAPCRACK3D), are available.

Cohesive elements and surfaces

In cases where the crack propagation path can be pre-defined, interface elements can be placed along the crack path (Needleman, 1990). A typical formulation is to use traction-separation type cohesive zone models (see Chapter 2.2.2) for the interface. The crack propagates after sufficient stress is reached in front of the crack and a predefined amount of energy is dissipated. Zero-thickness interface elements and finite thickness cohesive elements are available for this purpose in major FE codes. The sole purpose of such elements is to model

the softening in front of a crack and the whole model cannot be comprised of these elements alone. If the crack propagation path is unknown, potential propagation paths must be defined everywhere in the model, i.e. between all normal elements (Xu and Needleman, 1994). Publication IV uses such an approach. The drawbacks are the vastly increased computational effort and the mesh-dependency of the fracture propagation, which can be alleviated by a careful design of the mesh topology (Tijssens et al., 2000).

Element erosion and node release

Typically with quasi-brittle materials, the crack initiation location and propagation path are not known *a priori* and the material fractures in the location determined by a constitutive model. The most common approach to accommodate the finite element mesh to the damage is to remove (erode) the elements that have lost their load-bearing capacity from the model (Song et al., 2008). This introduces a free surface that can contact other free surfaces in the model, converting the internal damage into a discrete fracture. While it is fairly straightforward to implement, the approach violates the conservation of mass, creates a discrete fracture which is dependent on the mesh size and can cause an imbalance in stresses if the removed element was not completely softened in all directions. Related to the element erosion approach is the node release technique, in which a node shared by several elements is duplicated or a bond tying two coincident nodes together is broken so that the elements utilizing the previously common node are fully separated from each other at this location (Xie and Biggers, 2006). The approach can be utilized like the interface elements described above with pre-defined fracture paths, or at any element interface experiencing sufficient nodal forces (Camacho and Ortiz, 1996). The approach adopted in Publication IV utilizes element erosion, but not in the traditional sense of removing bulk elements from the analysis but by removing the failed interface elements that are small compared to the bulk elements.

Other methods

A large number of methods not mentioned above have been proposed to model different phases of the quasi-brittle failure process. Notable examples include methods based on the internal representation of the discontinuity within the element formulation, discrete and boundary-based methods and meshless methods (Mohammadnejad et al., 2018). Many of the proposed methods have been tailored to address a particular phase of the failure process. For example, the extended finite element method (XFEM) utilizing enriched element shape functions to include the discontinuity in the model tracks the crack growth path accurately using fracture mechanics criteria but has problems in representing complex crack shapes, branches or resulting fragmentation (Sukumar et al., 2015). Moreover, some of the more recent techniques have not evolved to a point where a ready to use implementation is made available to the public. The other techniques are not discussed here in more detail as they were not applied in the current work. A recent thorough review of the techniques is given by Mohammadnejad et al. (2018).

Summary

Different kinds of techniques have been developed to model discrete fracturing and selecting the most feasible technique largely depends on the case to be modelled. Various applications of the cohesive zone models combined with finite elements appear to be the most popular if the focus is in capturing the initial phases of the failure process, from the initiation of the cracking to crack coalescence and macroscale failure. The discrete techniques capture the post-failure process and subsequent failures more robustly. Publications III and IV discussed in Chapters 3.3 and 3.4 present the developments aiming to bridge the gap between the continuum damage and discrete cracking.

3. Developed modelling methods

This chapter describes the modelling methods, which were developed and applied to study the failure process of quasi-brittle materials in this thesis. Each of the following sections presents a technique developed to capture one of the four phases of the failure process dissected in Figure 2. A brief background of modelling approaches was presented in Chapter 2.2. The modelling results of the different phases of the failure process are presented in Chapter 4.

3.1 Effects of microcracks before crack growth

This section addresses the first phase of the numerical modelling of the failure process of quasi-brittle materials (Figure 2). As discussed in Chapter 2.1, the initiation of cracks, their interaction and coalescence play a significant role in the failure of both brittle and quasi-brittle materials. The first phase of the failure process in Figure 2 includes the representation of the microcracking in the material and its effects on the continuum response and susceptibility to fracture onset, before the first crack growth.

The interaction of microcrack arrays in an otherwise elastic material was studied in Publication I. The study was made by combining fracture mechanics to model the behaviour of the internal cracks with the finite element method to homogenize the microcrack responses over the continuous domain. The specific methods used in the study are outlined below.

As discussed in Chapter 2.1, quasi-brittle materials typically contain numerous defects that propagate and adjoin to cause a macroscopic failure. The behaviour of each microcrack is driven by the stress state in the vicinity of the crack. The stresses are mainly due to external loading, but the neighbouring cracks can affect each other considerably, altering the loading subjected to the cracks by the far-field stresses. The interaction effects can be amplifying, if the cracks are located in the tensile zones of each other's stress fields, or shielding if they induce compression onto each other (Kachanov, 2003). Analytical SIF solutions exist for different crack interaction systems, but also the principle of superposition can be applied to solve the behaviour of the crack array.

Method for solving crack interactions

In Publication I, a combined analytical-numerical method was developed for solving the interaction of the cracks and for studying how the cracks affect the

continuum behaviour of the material. The method is a combination of an analytical approach to solve the interaction between the microcracks and a numerical finite element (FE) based method to homogenize the microcrack response to the continuum scale. The behaviour of the cracks is described using linear fracture mechanics (Chapter 2.2.1).

The interactions between the microcracks are solved by the linear superposition-based method developed by Kachanov (1987). The method was originally developed to model the interaction of internal cracks but it was expanded to consider also edge cracks in Publication I.

In the method, a linear system of equations is formulated for the crack array in an elastic solid and the solution yields the tractions subjected to each crack considering the mutual interactions of the cracks. The key assumption of the method that yields the linear system of equations is that the variation of the stress fields caused by a crack along its neighbours can be neglected, and only the averaged effects from one crack to another need to be considered. Kachanov (1987) argues that this simplification gives results of high accuracy when the cracks do not vary in length significantly. The linear system of equations is constructed by assuming normal and shear stresses of unit intensity on each crack and by calculating the induced average stresses over each crack in the normal and shear directions. This provides the constant coefficients in the equation system, denoted as the transmission factors. Then, by considering the magnitude of the average stress at each crack as unknown, the following system of equations is obtained:

$$\begin{aligned} p_i^* &= p^{ext} + \sum_{\substack{j=1..N \\ j\neq i}} \left(\Lambda_{ij}^{\mathrm{pp}} p_j^* + \Lambda_{ij}^{\mathrm{tp}} t_j^*\right) \\ t_i^* &= t^{ext} + \sum_{\substack{j=1..N \\ j\neq i}} \left(\Lambda_{ij}^{pt} p_j^* + \Lambda_{ij}^{tt} t_j^*\right) \end{aligned} \tag{4}$$

The system is solved for the unknown normal and shear stress averages p_i^* and t_i^*, by Gaussian elimination, for example. N is the total number of cracks in the system. The Λ terms are the transmission factors, which only need to be calculated once based on the mutual positions of the cracks. These are calculated separately for both the normal stress and shear stress, based on the analytical LEFM solutions of the standard stress fields, i.e. the stress fields caused by an isolated crack under uniform loading in an infinite body. These stress fields can be obtained by using the Westergaard stress function method, for example, or they can be found in numerous textbooks. Specifically, an internal through-thickness crack with the length $2l$ in an infinite plate under uniform tension induces the following normal and shear stresses at point P (Sun and Jin, 2011):

$$\begin{aligned} \sigma_{xx}(P) &= \frac{\sigma_0 r}{\sqrt{r_1 r_2}}\left[\cos\left(\theta - \frac{1}{2}\theta_1 - \frac{1}{2}\theta_2\right) - \frac{l^2}{r_1 r_2}\sin\theta \sin\frac{3}{2}(\theta_1+\theta_2) - \frac{\sqrt{r_1 r_2}}{r}\right] \\ \sigma_{yy}(P) &= \frac{\sigma_0 r}{\sqrt{r_1 r_2}}\left[\cos\left(\theta - \frac{1}{2}\theta_1 - \frac{1}{2}\theta_2\right) + \frac{l^2}{r_1 r_2}\sin\theta \sin\frac{3}{2}(\theta_1+\theta_2)\right] \\ \sigma_{xy}(P) &= \frac{\sigma_0 r}{\sqrt{r_1 r_2}}\left[\frac{l^2}{r_1 r_2}\sin\theta \sin\frac{3}{2}(\theta_1+\theta_2)\right] \end{aligned} \tag{5}$$

The point P is defined in a cylindrical coordinate system with the origin at the crack centre point as visualized in Figure 12. Directly ahead of the crack tip, the stress fields reduce to their near-tip forms. For example, the stress field normal to the crack reduces to a form which is only dependent on the distance from the crack tip and the stress intensity factor K_I: $\sigma_{yy}(r_1, \theta_1 = 0) = \frac{\sigma_0\sqrt{\pi l}}{\sqrt{2\pi r}_1} = \frac{K_I}{\sqrt{2\pi r}_1}$. It is important to note that the near-tip fields rapidly lose their accuracy further away from the crack tip and the full stress fields are needed for evaluating the transmission factors correctly. A similarly formulated stress field solution is given for the shear loading on the crack by Sun and Jin (2011).

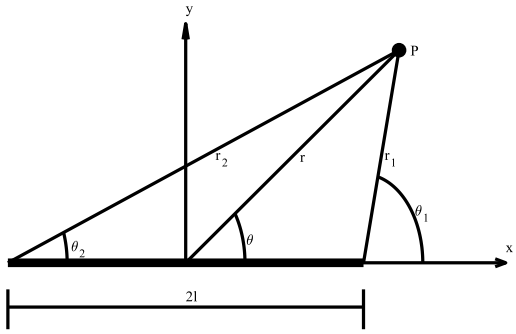

Figure 12. Definition of the internal crack stress field coordinates to evaluation point P (Eq. 5).

The method for solving interactions by Kachanov (1987) was extended to take into account edge cracks. Concise closed-form solutions for the stress fields are not available for edge cracks and the fields were determined via FE simulations in Publication I. The validity of these stress fields was confirmed by fitting the analytical series form solutions to the FE results as shown in Figure 13.

The method maintains its accuracy if the crack lengths in the system do not vary significantly. However, it may be of interest in some cases to consider the effects of smaller cracks on a larger one. An example of such a case is a macroscopic crack in a quasi-brittle material with a fracture process zone consisting of microcracks. The technique developed for Publication I allows such assessments if the macroscale crack is represented by the element boundaries and the microcracks within the material model. The micro-macro interaction effects are captured by calculating the additional tractions induced by the microcracks on the macrocrack faces while the macro-micro interaction effects are the natural result of the finite element model.

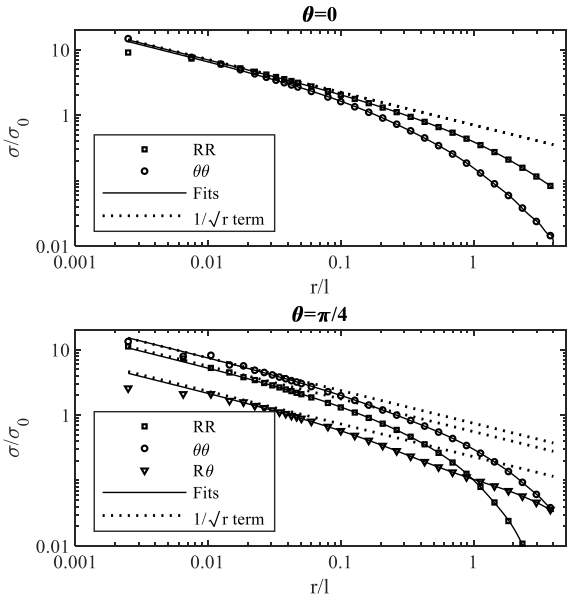

Figure 13. Series form stress solutions fitted to the simulated stress fields in a cylindrical coordinate system caused by an edge crack in an infinite plate under remote tension.

Crack closure and friction

As the microcracks in quasi-brittle materials can be randomly oriented and also induce compressive stresses in the material, the crack closure effects need to be considered for an accurate assessment of the crack interactions and the effects of microcracks on the continuum softening. The method developed for Publication I includes the effects of crack closure and the friction between closed crack faces. This extension changed the solution of the interaction system from a linear to nonlinear solution. In the case of crack face contact for any of the cracks in the system, the solution had to be sought iteratively. A linear predictor was first calculated, and contact stresses were slowly ramped up on the overlapping crack faces until the overlap was removed and the system was in equilibrium. Frictional stresses due to Coulomb friction, which reduces the effects of the external shear stresses, were induced in the process. As a result, a closed and fully sticking crack behaved as if it was not present in the system.

Crack opening displacements and RVE homogenization

In Publication I, a material model was developed for capturing the effects of the microcracking on a continuum scale. After the solution of the interactions, the microscale crack behaviour was homogenized into continuum softening effects, which are denoted as damage in Chapter 2.2.2, by adopting a representative volume element (RVE) based approach. RVE is a concept that estimates the average properties of inhomogeneous materials by averaging the strains induced by the discontinuities in the material. An RVE has to be large enough to contain a statistically sufficient number of inclusions so that its response can be captured via uniform macroscopic stresses and strains (Gitman, 2006).

The discontinuities within the RVE contribute to the average strains. For example, for a volume of material with crack-like features, the crack-induced strains can be deducted from the decomposition of the overall strain tensor. In a 2-D setting, consider an area A visualized in Figure 14 containing i=1..N cracks with lengths $2l^i$, normals $\vec{n}^i$ and crack opening displacement vectors $\vec{b}^i$. By integrating the strain tensor over the area A separately for the matrix surrounding the cracks and the crack lines, and by using the divergence theorem, a convenient decomposition of the total strain into the elastic matrix strains, ϵ^{el}, and strains induced by the crack openings, ϵ^{cr}, is obtained (Kachanov, 1993):

$$\epsilon = \epsilon^{el} + \epsilon^{cr} = \mathbf{M^0}\colon\boldsymbol{\sigma} + \frac{1}{2A}\sum_i(\vec{b}^i \otimes \vec{n}^i + \vec{n}^i \otimes \vec{b}^i)\, 2l^i, \tag{6}$$

where the elastic strains in the matrix are defined normally with the applied stress $\boldsymbol{\sigma}$ and the elastic compliance $\mathbf{M^0}$. It was assumed that the normal vectors and the crack opening vectors are constant over the crack planes.

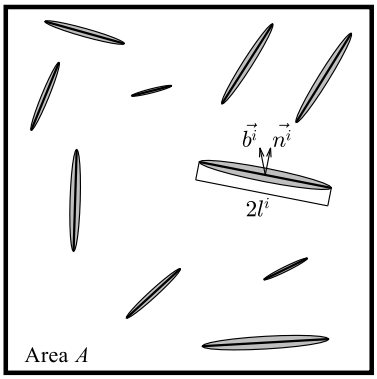

Figure 14. A schematic example of a 2-D RVE with internal cracks with lengths $2l^i$ normals $\vec{n}^i$, crack opening displacement vectors $\vec{b}^i$ and an elliptical crack opening shape.

If the opening of the cracks can be expressed directly as a function of the external load, a total stress-strain relationship can be deducted from Eq. (6). Such a case occurs if the planar cracks do not interact. The crack opening displacement vector for a non-interacting internal crack of length $2l^i$ subjected to stress $\boldsymbol{\sigma}^i$ or crack face traction $\vec{t}^i$ can be written as (Kachanov et al., 2003)

$$\vec{b}^i = \vec{n}^i \cdot \boldsymbol{\sigma}^i \cdot \mathbf{B} = \vec{n}^i \cdot \boldsymbol{\sigma}^i \cdot \frac{\pi l^i}{E_0/(1-\nu^2)}\mathbf{I} = \frac{\pi l^i}{E_0/(1-\nu^2)}\vec{t}^i, \tag{7}$$

where the crack opening tensor $\mathbf{B}$ was taken as its 2-D plane strain form and E_0 and ν are the elastic constants for the matrix. In the case with crack interactions, the crack face traction vector $\vec{t}^i$ is obtained by solving the crack interaction system equations (Eq. 4). Moreover, the edge cracks also included in the crack arrays open differently to the internal cracks. The handbook solutions for edge cracks (Tada et al., 2000) indicate that the average opening of an edge crack is higher by a factor of 1.258 than the opening of a corresponding internal crack.

After the solution of the interaction system and the crack opening displacements (Eqs. 4 and 7), the effective elastic properties can be determined via the elastic potential and the strain decomposition (Eq. 6) as:

$$f(\boldsymbol{\sigma}) = \frac{1}{2}\boldsymbol{\sigma}\colon(\boldsymbol{\epsilon}^e + \boldsymbol{\epsilon}^{cr}) = \frac{1}{2}\boldsymbol{\sigma}\colon\mathbf{M}^0\colon\boldsymbol{\sigma} + \frac{1}{2A}\sum_i\,(\vec{n}^i \cdot \boldsymbol{\sigma} \cdot \vec{b}^i)l^i\,, \tag{8}$$

from which the total compliance tensor is obtained as

$$\boldsymbol{M} = \frac{\partial f(\boldsymbol{\sigma})}{\partial \boldsymbol{\sigma}} = \boldsymbol{M}^0 + \frac{1}{2A}\frac{\partial}{\partial \boldsymbol{\sigma}}\sum_i (\vec{n}^i \cdot \boldsymbol{\sigma} \cdot \vec{b}^i) l^i \quad (9)$$

A compliance matrix of the material is required for the finite element solver to find the next converged solution. Due to the possible nonlinearity induced by the crack closure and friction, the compliance can change as the load is being applied to the system. In the calculation cases of Publication I, it was found that the elastic compliance approximated the tangent stiffness well enough for the calculations to converge rapidly without costly numerical approximations of the actual compliance at each calculation increment.

The arrays of microcracks considered in the study were constructed independent of the finite element mesh topology, meaning that the cracks were not associated with any specified element integration points. As a result, the cracks cross element boundaries and their constitutive contributions need to be spread over a finite area. A spatial RVE-type regularisation model was used for this purpose (Bažant, 1991). According to the regularisation, the average crack induced strain, $\bar{\boldsymbol{\epsilon}}^{cr}$, at material point $\mathbf{x}$ is the sum of the strains caused by one or more cracks at points $\boldsymbol{\xi}$ in the vicinity of $\mathbf{x}$:

$$\bar{\boldsymbol{\epsilon}}^{cr}(\mathbf{x}) = \int_A \alpha(\mathbf{x}, \boldsymbol{\xi})\, \boldsymbol{\epsilon}^{\mathbf{cr}}(\boldsymbol{\xi}) \boldsymbol{d\xi}, \quad (10)$$

where α is the influence function. The calculations in Publication I applied a Gauss distribution type function with an influence radius r_0:

$$\alpha(r) = \begin{cases} \exp\left(-\frac{1}{1-\left(\frac{r}{r_0}\right)^2}\right), r < r_0 \\ 0, r \geq r_0 \end{cases}, \quad (11)$$

where r is the distance between the assessment point and the centre point of the crack. The influence function is also normalised so that the total crack strain generated at the crack point is accumulated within the influence radius. The homogenization effectively increases the RVE area while maintaining the spatial element resolution needed to capture the stress gradients. The correct selection for the influence radius depends on the size of the discontinuities located inside the RVE. The radius needs to be large enough to capture a statistically representative number of inclusions within the RVE.

Equations (6-11) complete the definition of the material model needed to capture the microcrack responses in a continuum scale.

Stress intensity factors and the onset of fracture

The growth potential of the microcracks and the onset of macroscopic fracture can be assessed using the stress intensity factor. As the calculations of Publication I modelled the response of fixed, or non-propagating, crack systems, the stress intensity factor had only an output-type purpose in the calculations but was essential in quantifying the interaction effects. The interaction between the cracks and their effects on the continuum stiffness were defined using the crack face tractions and crack opening displacements as outlined above.

For the internal cracks in the material, an approximation of the Mode I stress intensity factor can be obtained from the average traction p^* acting on the crack as (Anderson, 2017):

$$K_I = p^* \sqrt{\pi l}, \quad (12)$$

where l is the crack length. The effects of the neighbouring cracks cause the crack face traction to vary along the crack face, which requires the application of the weight function technique to obtain the correct stress intensity factors at both tips of the crack (Anderson, 2017, Ch. 2.6.5). The weight function technique is also required for the edge cracks in the system but using a different weight function than for the internal cracks.

The results of the calculations in Publication I, summarized in Chapter 4.1, use the changes in the values of the stress intensity factors as a means to assess the amplification and shielding effects due to the crack interaction.

Implementation

The method was implemented within the commercially available FE code Abaqus (Abaqus, 2017) with Fortran user subroutines, by assuming 2-D plane strain conditions and using linear four-node elements. The opening of the microcracks has a directional softening effect on the local constitutive behaviour, which was calculated within the UMAT subroutine in Abaqus. The global crack interaction aspects, stress intensity factor calculation and the RVE homogenization were determined via the UEXTERNADB routine. Abaqus calls the subroutines and processes information in an order, which required that the crack system solution to utilize the Euler forward solution scheme, in which the crack interactions are solved only after each element is processed during the time increment. The crack opening displacements and homogenized crack strains calculated at the end of the increment are used as the initial conditions for the next time increment. This requires that the external loads are ramped up slowly to allow the crack system and FE solution to converge at the same pace.

Applicability and limitations

The primary application of the method is in cases where the defect density is relatively high and the defects are several orders of magnitude smaller than the structural scale, making it unfeasible to consider modelling each defect individually. The approximation used in the superposition of the cracks requires that the defect sizes do not vary significantly.

In the current implementation, the cracks have to be idealised as linear due to the utilisation of the fundamental crack stress field solutions. More complex crack shapes can be considered with the superposition principle by dividing the crack profiles into linear segments and assuming that the resulting stress fields remain elastic. Approaches of this type have been used to predict crack growth in rock masses (Crouch 1976; Shi et al. 2014). The coupling between the fracture mechanical and continuum solution requires that the crack opening displacements and stress intensity factors need to be available from the crack calculations. Similarly, the approach could be extended to consider the effects of pores and inclusions in the matrix with appropriate stress field solutions.

Due to the assumption of elasticity in the matrix behaviour and the stress fields caused by the individual defects, the method is independent of scale. The elastic assumption limits the applicability to cases where the material behaviour is brittle or that the defects remain stationary. It can be extended to consider

crack propagation as long as the crack growth does not include significant energy dissipation, which causes inelasticity and violates linear superposition and the ideal stress field solutions used to calculate the interactions between the cracks. Therefore, the method cannot model the interaction of several cracks with a large fracture process zone. Similarly, other inelastic deformation mechanisms in the matrix, such as creep, cannot be captured with the elastic stress field solutions.

The simultaneous evaluation of the crack interaction solution and the finite element solution allows for the method to be applied to different geometries rapidly. The current implementation was made assuming a 2-D setting, but an extension to 3-D can be made using the same principles.

3.2 Growth of microcracks into a macroscopic failure

As discussed in Chapter 2.1, the initiation of cracks, their interaction and coalescence play a significant role in the failure of both brittle and quasi-brittle materials. The growth, interaction and coalescence of the internal defects belong to the second phase of the failure process shown in Figure 2, as well as the prediction of the first macroscopic failure. The methods developed to capture this phase are presented in this section.

The confined compressive failure of an inhomogeneous brittle material containing initial defects was studied as an example of this phase in Publication II. The study was performed primarily by using fracture mechanics to model the behaviour of the internal cracks. The specific methods used in the study are outlined below after a brief description of the assumed wing crack failure mechanism.

Compressive failure by wing crack coalescence

As discussed in Chapter 2.1, the fracture of quasi-brittle materials under compression can be caused by the growth and coalescence of pre-existing flaws. As the compressive load is increased, the existing main cracks in various orientations inside the material undergo sliding deformations and small extensions to the main crack start growing at an angle with respect to the main crack orientation. The growth tends to turn towards the direction of the maximum principal stress, splitting the specimen axially (Renshaw and Schulson, 2001). If there are laterally acting compressive stresses, i.e. confinement, the crack growth can be arrested, but increasing the primary compression may lead to a failure mode that macroscopically appears as a shear band, inclined with respect to the principal loading direction. This type of failure in brittle materials has been attributed to be caused by the coalescence of smaller closely-packed cracks (Horii and Nemat-Nasser, 1985).

The axial splitting can be represented using a wing crack model (Lehner and Kachanov, 1996). Such models consider a pre-existing main crack, oblique to the loading direction, which experiences sliding deformation due to the compressive loads. Small extensions, wings, form at the two ends of the main crack. Multiple secondary cracks have also been observed to form along the main crack in ice and rock (Bobet and Einstein, 1998; Schulson et al., 1999). The wing crack

configuration is visualized in Figure 15a. The sliding of the main crack faces against each other creates Mode I conditions in the wings, which start to extend in a stable manner. The extension of a wing crack is stable because the extension of the wings requires an increase in the external loading. It is further postulated that there exist adjacent main cracks that link together to cause a macroscopic axial splitting failure. With lateral confinement, the crack closure stresses induce friction on the main crack faces. If the main crack is sufficiently large, the frictional stresses can prevent the sliding of the crack faces against each other, arresting the crack growth.

Experimental observations on brittle materials suggest that under sufficient confinement, the failure mode changes from axial splitting to a shear-like fault (Bažant and Xiang, 1997), as visualized in Figure 4. Experiments performed with transparent materials with pre-fabricated cracks confirm that the macroscopic shear fault can be caused by the coalescence of suitably oriented and closely-spaced smaller cracks (Horii and Nemat-Nasser, 1985). Larger, but isolated, cracks are arrested by the confinement, but the densely packed small cracks can grow, helped by the interaction between the cracks.

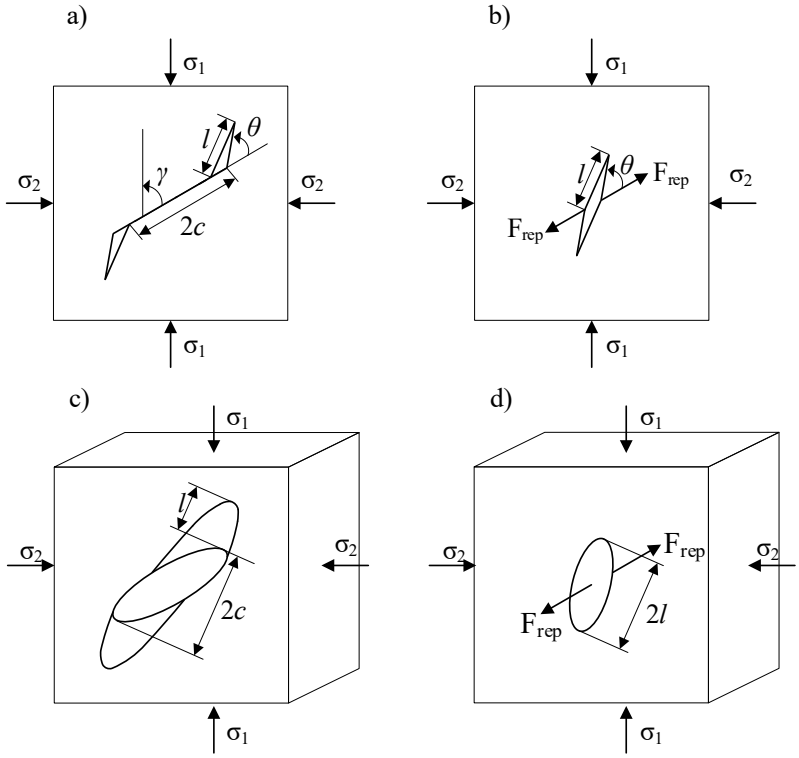

Figure 15. An idealization of a wing crack with its extensions in 2-D (a,b) and 3-D (c,d). The pre-crack of size $2c$ extends by length l due to the main compression σ_1 and lateral confinement σ_2.

The shear faulting mechanism outlined above has been validated experimentally in a 2-D setting (Horii and Nemat-Nasser, 1985). The study in Publication II aimed to extend this assessment by evaluating whether such behaviour is pos-

sible also in 3-D, i.e. whether the coalescence of suitably oriented and neighbouring small penny-shaped main cracks in an infinite medium can cause a macroscopic failure also when there is lateral confinement. Experimental evidence of 3-D wing cracks under uniaxial compression suggest crack arrest for isolated cracks but a set of suitably oriented cracks were able to produce a complete fracture of the specimen (Dyskin et al., 2003).

Method for solving wing crack interaction and propagation

The calculations in Publication II study the periodic arrays of main cracks in 2-D and 3-D geometries shown in Figure 23. The study assumes that the cracks propagate via the wing-crack mechanism outlined above and visualized in Figure 15. A key ingredient in the solution is the interaction between the cracks, which helps the otherwise arrested cracks to grow.

It has been shown that the wing cracks can be idealized as straight cracks and the sliding of the pre-crack faces can be taken into account with additional loads on the idealized cracks (Basista and Gross, 2000; Dyskin et al., 1999; Horii and Nemat-Nasser, 1985). This idealization is visualized in Figure 15. The representative loads acting on the idealized cracks can be deduced from the wing crack kinematics as follows. The stress subjected to the idealized cracks is the sum of the external load and the force due to the frictional sliding of the main crack distributed over its length:

$$\sigma_{rep}^{N} = \vec{n} \cdot \frac{\vec{F}_{init} + \vec{F}_{rep}}{\pi l^2} \text{ and } \vec{\tau}_{rep} = \frac{\vec{F}_{init} + \vec{F}_{rep}}{\pi l^2} - \sigma_{rep}^{N} \vec{n} \tag{13}$$

The sliding force of the main crack due to the frictional stress is:

$$\vec{F}_{init} = \pi c^2 < \|\vec{\tau}_{init}\| - \tau_{\mu,init} > \frac{\vec{\tau}_{init}}{\|\vec{\tau}_{init}\|} \text{ where } \tau_{\mu,init} = \mu < -\sigma_{init}^{N} > \tag{14}$$

and the main crack stresses are the projection of the stress state onto the idealized crack:

$$\sigma_{init}^{N} = \vec{N} \cdot \boldsymbol{\sigma} \cdot \vec{N} \text{ and } \vec{\tau}_{init} = \vec{N} \cdot \boldsymbol{\sigma} - \sigma_{init}^{N} \vec{N} \tag{15}$$

Above, Macaulay brackets < > were used and $||\cdot||$ denotes the vector norm.

Similar to the approach utilized in Publication I, the interaction of the flaws was solved in Publication II by using the simple method developed by Kachanov (1987). The 3-D version of the equation system used to solve the unknown average traction vector components acting on the cracks is:

$$\begin{aligned} p_i^* &= p^\infty + \sum_{\substack{j=1..M \\ j \neq i}} \left(\Lambda_{ij}^{\mathrm{pp}} p_j^* + \Lambda_{ij}^{\mathrm{tp}} t_j^* + \Lambda_{ij}^{\mathrm{sp}} s_j^* \right) \\ t_i^* &= t^\infty + \sum_{\substack{j=1..M \\ j \neq i}} \left(\Lambda_{ij}^{\mathrm{pt}} p_j^* + \Lambda_{ij}^{\mathrm{tt}} t_j^* + \Lambda_{ij}^{\mathrm{st}} s_j^* \right) \\ s_i^* &= s^\infty + \sum_{\substack{j=1..M \\ j \neq i}} \left(\Lambda_{ij}^{\mathrm{ps}} p_j^* + \Lambda_{ij}^{\mathrm{ts}} t_j^* + \Lambda_{ij}^{\mathrm{ss}} s_j^* \right) \end{aligned} \tag{16}$$

In these equations, p_i^* is the normal stress and t_i^* and s_i^* are the two shear stresses on the crack i plane, and M represents the number of cracks. The problem reduces to a system of $3M$ linear equations, from which the unknown tractions p_i*, t_i* and s_i* can be solved.

As with the method utilized in Publication I, the transmission factors Λ were calculated based on the standard stress fields, either for a 2-D line crack or a 3-D penny-shaped crack, assuming LEFM conditions. The cracks were allowed to propagate in the calculations, requiring the transmission factors to be recalculated for each considered increment. Moreover, the effects of crack face contact and friction were included in the crack interaction solution using the Coulomb friction model, which necessitated the use of a nonlinear solution method for the equation system.

Contrary to the approach in Publication I, which assumed fixed crack configurations, the stress intensity factor now plays a key role in controlling the growth of the cracks in the system. The stress intensity factors were calculated with the weight function method (Anderson, 2017, Ch. 2.6.5) using the crack face tractions resulting from the interaction calculations. Once the specified critical value of the stress intensity factor was reached, the crack was assumed to propagate by a small increment in the most susceptible direction. The principle of minimum potential energy implies that a crack seeks a growth path resulting in the maximum energy dissipation, i.e. the maximum energy release rate, which also corresponds to the maximum Mode I stress intensity factor (Anderson, 2017, Ch. 2.11). Accordingly, the prediction of the propagation direction was made by considering an infinitesimal increment of the crack with an unknown angle and finding the direction that maximizes the Mode I SIF.

Implementation

The calculations in Publication II considered differently oriented periodic crack arrays with a size of 11×11, which was determined to provide a converged solution for approximating the response of an infinite periodic crack array (see Table 2 of Publication II). The main crack midpoints were assumed to be located on the same plane, but the cracks were not typically aligned with the plane adjoining the crack centre points. The orientations most susceptible to unstable fracture were sought in the calculations. The calculations were performed by using Matlab and the *fsolve* and *fminsearch* root finding and minimization functions, respectively. The calculations focused on the growth behaviour of the individual cracks and the continuum homogenization used in Publication I was not required. Consistent with the aims of this thesis, the fracture mechanical description of the crack array and its growth behaviour could be utilized as a part of a finite element method compatible constitutive model of a quasi-brittle material under compression, if augmented suitably with the description of the elastic response of the material and a continuum homogenization of the defects.

Applicability and limitations

The developed method models the unconfined and confined compressive failure of an infinite continuum assuming periodic initial defect patterns. The purpose was to consider a scenario where the structural dimensions greatly exceed the crack dimensions and the regular internal structure, such as repeating grains in ice, enables periodic defect patterns. Different periodic and non-periodic defect patterns can be studied with the method easily.

A wing crack model was applied to describe the defects, which were then idealised as penny-shaped cracks for the crack interaction calculations. The superposition principle is compatible with a finer discretization routine of the crack shapes but it would increase the degrees of freedom in the solution considerably (Crouch, 1976).

As in Publication I, an elastic behaviour was assumed for the stress fields and the matrix material. This limits the applicability to cases where the deformation and failure occur by crack growth, i.e. the brittle regime. Other inelastic deformation mechanisms, such as creep, violate both the elastic assumption and the principle of superposition. Renshaw and Schulson (2001) show how the deformation mechanism becomes ductile in compression if the sliding of the internal flaws is suppressed. The current implementation predicts infinite strength in such cases as ductile behaviour is not included in the model.

3.3 Discretization of fracture

The third phase of the quasi-brittle failure process of Figure 2 is addressed in this section. This phase includes the discretization of the predicted macroscopic fracture in the material. This is realized by converting the adjoined microcracks, or damage predicted otherwise, into an explicit fault in the numerical model.

A remeshing method for discretizing the damage predicted by the continuum material model was developed in Publication III for this purpose. The method was designed to be compatible with common finite element software without specific requirements for the material behaviour, other than the capability to predict a failure plane within the material. The details of the developed method are outlined below. In short, the developed approach is a 3-D “delete-and-fill” approach for the finite element framework, based on a simple element splitting technique to introduce the discontinuity in the finite element mesh, similar to that proposed by Bremberg and Dhondt (2009). The discontinuity is introduced in the mesh by removing the damaged element and filling its volume with smaller elements that contain the discontinuity.

Softening model

A prerequisite for introducing an explicit fracture in the mesh is that the plane of the fracture needs to be free of stresses. In Publication III, this was obtained with a simple fictitious crack material model. Different types of damage mechanics models could be applied to describe the softening of the material and to yield a more accurate continuum representation of the quasi-brittle failure process. However, the focus of Publication III was the remeshing method and not the on the development of a sophisticated fictitious crack model. The feasibility of the approach was demonstrated using a simplified damage model that results in a stress-free plane within the continuum mesh.

A simple strain-based anisotropic material model is adopted in the work. In the model, the damaging process follows the evolution of the maximum principal strain. The constitutive relation was formulated directly in the principal strain directions as:

$$\begin{bmatrix}\sigma_1\\ \sigma_2\\ \sigma_3\end{bmatrix} = \frac{E}{(1+\nu)(1-2\nu)}\begin{bmatrix}(1-D)(1-\nu) & (1-D)\nu & (1-D)\nu\\ (1-D)\nu & 1-\nu & \nu\\ (1-D)\nu & \nu & 1-\nu\end{bmatrix}\begin{bmatrix}\epsilon_1\\ \epsilon_2\\ \epsilon_3\end{bmatrix}, \quad (17)$$

where E is the elastic modulus, ν is the Poisson ratio and D is the scalar damage variable. The subscripts 1, 2 and 3 denote the principal directions. As the damage approaches unity, the model softens all contributions from the maximum principal strain in the associated stress direction as well as the lateral Poisson effects. The formulation of the model is similar to the simple rotating crack model presented by Bažant and Planas (1998, Ch. 8.5.6). Also other types of constitutive damage models, such as those described in Chapter 2.2.2, or explicit cracking models formulated in Chapters 3.1 and 3.2, could be adopted for the fracture prediction. The simple direct stress-strain formulation of Eq. (17) was used in Publication III to maintain the focus on the discretization aspects of the method.

In the softening model, the scalar damage variable D was adopted to quantify the magnitude and the effects of damage, without any attempt to tie the degradation to specific physical failure processes of the material. Instead, a fictitious crack-type softening formulation (see Chapter 2.2.2) was adopted in Publication III. After the onset of softening, a linear relation between the cohesive stress and separation over the fictitious crack plane was utilized. This is achieved by the following definition of the damage variable:

$$D = \frac{\delta_{fail}}{\delta_1}\frac{(\delta_1-\delta_{init})}{(\delta_{fail}-\delta_{init})}, \delta_{init} < \delta_1 < \delta_{fail}, \quad (18)$$

where δ_1 is the separation in the maximum principal strain direction, calculated from the strain and the characteristic element length, $\delta_1=\epsilon_1 L_{\text{char}}$. The characteristic length is typically the cubic root of the element volume. As shown in Figure 16, the damage initiates when $\delta_1=\delta_{\text{init}}$ and grows nonlinearly as a function of separation until the complete softening of the material in the direction of the maximum principal strain.

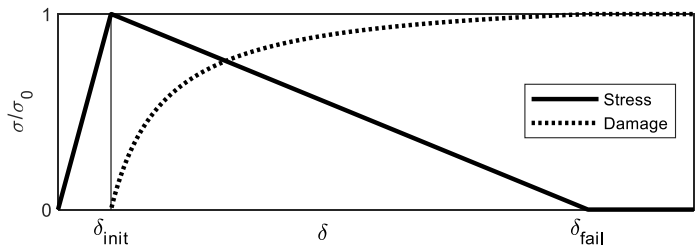

Figure 16. Stress-separation and damage behaviour of the simple fictitious crack model. As shown in Figure 7, the area under the curve is related to the fracture energy.

The stiffness degrades in the maximum principal direction, leaving the parallel directions unaffected. If the external loading direction varies, the applied model adjusts the damage orientation accordingly, which makes the model correspond with a rotating crack model and considers only Mode I conditions and the primary cracking associated with it. For simplicity, the model was formulated in the principal directions without considering that the directions may

change during loading. The directional softening of the stresses produces a completely traction-free plane inside the element that can be replaced with the free element faces in the remeshing process.

Remeshing procedure

Once the utilized damage model predicts that there would be a stress-free crack surface, the element containing that fictitious crack is replaced with several smaller elements filling the same volume but containing the predicted crack as external surfaces of the elements, as shown in Figure 17. The stress is relaxed in the principal strain direction, causing the normal of the stress-free plane to be oriented parallel to the principal strain direction. As shown in Figure 17, the method replaces one original element with eight smaller elements, four on each side of the crack, to obtain a more refined contact surface.

The equilibrium must be maintained during the modification of the finite element mesh. The kinematic and force balances in the solution were maintained by mapping the displacement, velocity and the stress and strain solutions to the newly created elements by using the shape functions of the original element. The mass balance was maintained by requiring the newly created elements to occupy the same space as the original element, i.e. that the newly created crack faces are not initially separated.

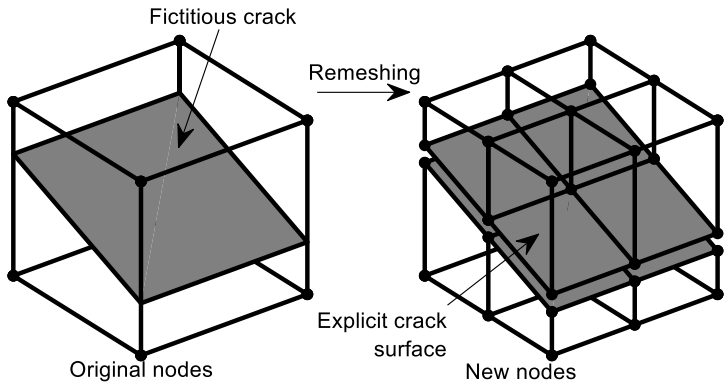

Figure 17. Conversion of an element with a fictitious crack into multiple elements with the crack as explicit free surfaces. Figure redrawn after Publication III.

Figure 17 depicts a rectangular element with a fictitious crack plane not coinciding with the node points of the element. In many cases, the element shape deviates from that of a right-angled rectangle, which may mean the softened element cannot be divided into two smaller elements of the same elementary shape, as visualized in Figure 5 of Publication III. However, not all irregular quadrilaterals (2-D) or hexahedrons (3-D) have unsuitable element geometries for use with the remeshing method, but only those with a significant kite-like shape. The implementation in Publication III aimed for simplicity and thus adjusted the orientation of the fictitious crack inside the original element to allow the division into smaller elements with the same elementary shape in the cases where the fracture was predicted in a poorly shaped element. This introduced a slight imbalance in the solution as the created free surfaces were not always

aligned with the stress-free plane. To minimise the disturbance to the solution caused by the remeshing, only the element containing the fictitious crack was remeshed. This introduced a non-confirming mesh boundary between the newly created elements and the original surrounding mesh, as seen in the examples presented in Chapter 4.3. The nodes of the new elements are located in the middle of the surfaces of the original elements. To tie the new elements with the existing mesh, interface elements were introduced in the mismatching interfaces. The need to use the interface elements could be removed by a finer remeshing routine.

Implementation

The remeshing approach was designed to alter the mesh topology so that the fictitious crack predicted by the continuum damage model in an internal material point is explicitly represented with the free boundaries of the finite element simulation model and that the approach is compatible with the FE software Abaqus. The requirement that the approach should work in conjunction with commercial FE software enabled the qualified built-in modelling, solution and post-processing routines to be readily available and the majority of the research effort could be focused on developing the remeshing routine. The approach is suited for a reduced integration elements where the complete constitutive behaviour of an element is evaluated within a single integration point and there is only a single fictitious crack with a failure plane extending over the whole element. Thus, the implementation assumed linear reduced integration 3-D solid elements.

The use of Abaqus set some restrictions on how the procedure could be implemented. The finite element mesh could not be modified during the calculation and the analysis had to be stopped to perform the remeshing. The state of the calculation model was read into a self-programmed Python routine, where the remeshing and solution transfer into the modified model was performed. The new state of the model was then written as a standard Abaqus input file, which was executed in the normal fashion. The flowchart of the process is shown in Figure 18.

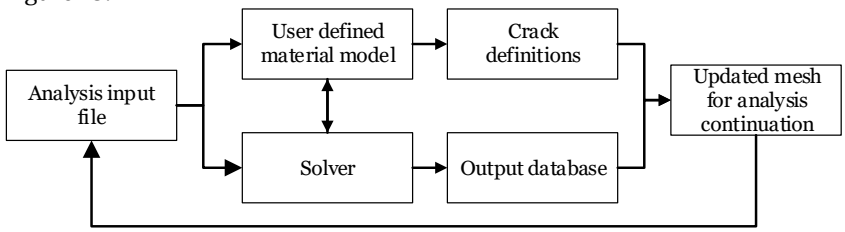

Figure 18. Flowchart of the remeshing process implemented on top of Abaqus FE software.

Applicability and limitations

The focus of the development was to capture the discrete features of the fracturing process. The current implementation makes use of a highly simplified damage softening model, which fulfils the requirements set by the remeshing approach, but does not capture the actual physics causing the fracture. As such,

the method predicts the fracturing behaviour of actual brittle and quasi-brittle materials mainly qualitatively at its current state. Augmenting the approach with a more sophisticated constitutive model is needed. The current constitutive model limits method to the brittle and quasi-brittle regime. Ductile fracture could be modelled, if a discrete surface can be predicted to occur due to the fracture.

The approach relies heavily on the other modelling capabilities provided by the finite element software. Therefore, the approach is easily applicable to any structural scenario where the behaviour is dominated by the initiation and growth of discrete fractures, both in 2-D and 3-D. Its application in a 3-D setting would allow for the proper consideration of the confinement effects on brittle fracture, which were found to be important in Publication II. Before attempting to make quantitative predictions, modifications need to be made in the constitutive model used in the simulation such that it represents accurately the internal fracturing process before the initiation of the first discrete crack.

In addition, some restrictions were set by the commercial finite element simulation code as discussed above.

3.4 Propagation of discrete failures

This section describes how the fourth phase of the quasi-brittle failure process of Figure 2 is addressed in this thesis and Publication IV. This phase includes the propagation of numerous discrete fractures through the material and representation of the post-failure behaviour of the quasi-brittle material.

To capture the multiphase failure process in complex loading cases, it is required that the topology of the numerical model can adapt to the predicted material point damage. As discussed in Chapter 2.2.4, this is traditionally achieved through the element erosion approach. In many cases, it is required that the fragments of the material separated by the failures remain in the simulations. Examples of such processes are the spalling and scabbing of a concrete plate during projectile impact (Figure 11) or the fragmentation of ice as it crushes against a structure (Figure 32). Particularly for ice, the separated fragments play an essential role in controlling how the failure propagates and which mode the failure takes as the crushing progresses. Therefore, a method that is more sophisticated than the element deletion approach is needed. The method in Publication III was designed to model the realistic propagation paths of a limited number of cracks in the material. Capturing the continuous fracturing process was found to be unfeasible for the method, particularly because of the remeshing limitations set by the Abaqus software (see the end of Chapter 3.3). This section outlines the improvements made to the technique for it to be applied to capture continuous fragmentation.

Cohesive surface methodology

A cohesive surface methodology was implemented to capture the fourth phase of the failure process in Figure 2. The method was applied to simulate the continuous crushing of an ice sheet in Publication IV. The work aimed to implement a method which would be able to model the continuous material fragmentation

process, including the interaction of the fragmented particles. The method utilized the fictitious crack model to predict the locations of the failures in the material and the finite element method together with cohesive elements to discretize the failures. The fundamentals of the technique had been presented in the literature, but ready-to-use implementations were not available. The techniques used in the study are outlined below.

A method denoted as the cohesive surface methodology (a term coined by Tijssens et al. (2000)) was implemented in Abaqus FE software and utilized to simulate the laboratory ice crushing experiments. Following the ideas of Tijssens et al. (2000) and Xu and Needleman (1994), breakable bonds were inserted between regular finite elements, which allowed the approach to capture the fragmentation of the crushing material and the subsequent interaction of the separated particles. Specifically, a finite element mesh was constructed by using bulk elements with unique nodes bonded together by interface elements (Figure 19). Abaqus FE software denotes these finite-thickness interface elements as cohesive elements. The failure of the interface elements created additional free surfaces in the model.

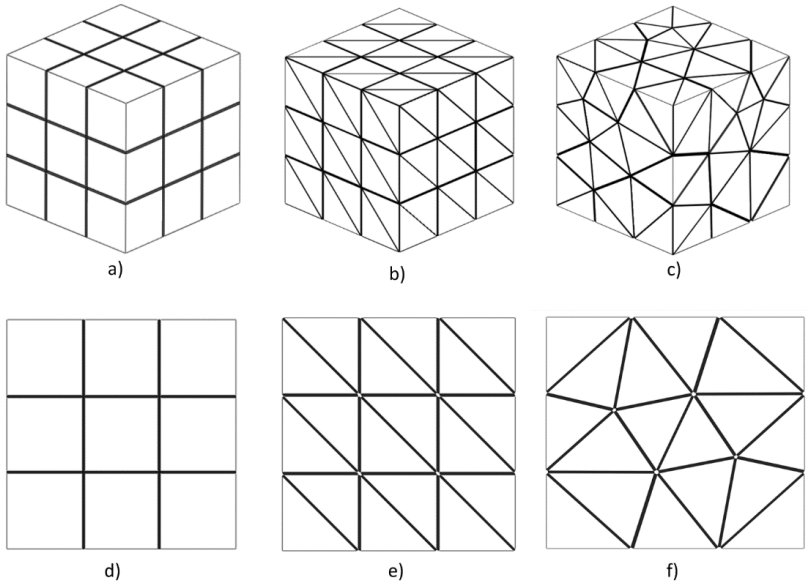

Figure 19. Joining of bulk elements together using cohesive elements at all interfaces in 2-D and 3-D structured and unstructured meshes. Figure adapted from Publication IV.

Due to numerical reasons, the cohesive elements were defined with a finite thickness instead of being perfectly planar. The interface thickness was set to be only a small fraction of the surrounding elements' thickness and removing them from the calculation had a negligible effect on the mass balance. The force balance was not affected as the elements are removed only after they are fully damaged, i.e. have lost all capacity to transmit loads across the interface. Tijssens et al. (2000) argue that a regular mesh, often best in traditional FE computations, is unsuited for capturing a complex and curved crack propagation path. The

aligned element edges prevent the crack path deviating from a straight line, as the path would need to change its direction perpendicularly. Tijssens et al., (2000) report that an unstructured mesh, similar to the one shown in Figure 199, is suitable when crack path curvature is expected. Therefore, an unstructured mesh was selected for the simulations in Publication IV.

The damage process was restricted only to the interface elements, making a fictitious crack parallel to the interface the only possible orientation, but the damage could be initiated by tensile loads (Mode I) or by in-plane shear loads (Mode II). Compressive loads are transmitted over the interface element in full, also after the failure of the interface element if the bulk element faces contact each other. Tensile and compressive loads parallel to the interface are carried by the adjacent bulk elements.

The simulations included frictional contact between all external surfaces, including the new surfaces, which are created as the interface elements fail and create fragments of the material. Additionally, gravity and buoyancy were included in the simulations. The simulations were performed using the Abaqus FE software using explicit time integration.

Applied softening models

A traction-separation law (see Chapter 2.2.2), which is a simple adaptation of the Hillerborg's fictitious crack model (Hillerborg, 1991), was specified to define the constitutive behaviour of the interface elements in the calculations. To evaluate their effects on the fracture process propagation and contact forces, different softening relations were tested. Linear, exponential and plastic-type stress-separation models shown in Figure 20 were applied in the calculations. The values of the softening model parameters could not be calibrated directly from the ice crushing experiments (Määttänen et al., 2011) modelled in Publication IV. Instead, strength and fracture energy values typical for ice were selected based on the literature (Dempsey et al., 2012; Timco and Weeks, 2010). The bulk elements were defined to use the ideal plastic von Mises model with the yield stress chosen based on the ice compressive strength measured during the experimental campaign (Määttänen et al., 2011). The failure process concentrates on the interface elements and the purpose of the bulk element plasticity is to limit the overall stresses to physical limits and provide a moderate amount of numerical stability through energy dissipation in the model.

Applicability and limitations

The implementation considers scenarios where the discrete failures occur locally in tension or shear. The model is limited to fracturing at locations predefined by the interface elements when the stress acting over the interface exceeds the defined strength. For simplicity, the implementation did not try to relate the internal microscale cracking process to the macroscale strength values used as the local failure model. The method is best suited in scenarios where the macroscopic tensile and shear cracking leads to fragmentation and keeping the separated fragments active in the simulation is an essential aspect of the process, such as in continuous crushing of an ice sheet under brittle conditions.

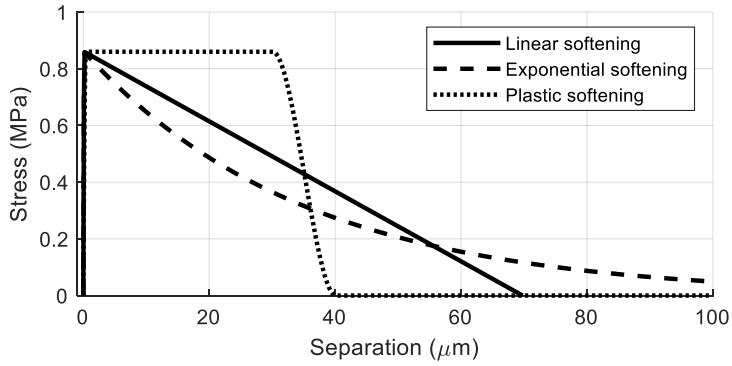

Figure 20. Different softening models applied in the simulations in Publication IV. The area under each curve equals 30 J/m^2.

The ice crushing process typically includes other mechanisms than brittle fracture, such as spalling and crushing at the contact zone that both occur both as brittle and ductile, depending on the deformation rate and the amount of confinement (Jordaan, 2001). This behaviour is not included in the model but the utilization of a finite element simulation software allows combining the model with a more sophisticated material model representing the true failure behaviour of the material. Some additional considerations need to be made on how to transfer the damage and softening occurring in the bulk of the material to the failure planes between the elements. This difficulty was aimed to be avoided by the remeshing procedure discussed in Chapter 3.3.

The implementation assumed a 2-D setting, although similar ideas can be utilised in 3-D. A 2-D model typically represents a thin slice at the mid-plane of the material. This yields a uniform out-of-plane confinement for the material. The results obtained in Publication II (Chapter 4.2) show that the 2-D idealisation is inaccurate if the process is naturally triaxial. The observations of the ice sheet brittle crushing process (Jordaan, 2001) suggest such features.

3.5 Application of the methods

This chapter summarized the methods presented in the publications included in this work. The next chapter presents example applications addressing each phase of the failure process of Figure 2. The methods are applied individually in separate case studies. The results of each phase are tied together in the concluding remarks in Chapter 5.

4. Modelling results

Chapter 3 presented the methods that were used to simulate the four phases of the failure process of quasi-brittle materials (Figure 2). This chapter summarizes the modelling results of each phase of the process. The results are presented in more detail in Publications I-IV. The presentation in this chapter is organized according to the phases. First, the modelling of the microcracking (Phase 1) is addressed in Chapter 4.1, followed by the findings made in the modelling of the macroscopic failure due to the internal cracking (Phase 2) in Chapter 4.2. Chapter 4.3 presents the simulations of the discretization of continuum damage (Phase 3) and the chapter ends with the results obtained with the technique used to transform microscale damage into explicit cracking (Phase 4, Chapter 4.4).

4.1 Interaction and softening effects of internal cracks

This section presents the modelling results of the microcrack behaviour and interaction in an otherwise elastic continuum. The calculations belonging to the first phase of the failure process of quasi-brittle materials (Figure 2) were performed using the method presented in Chapter 3.1. This phase includes the representation of the microcracking in the material and its effects on the continuum response and susceptibility to fracture onset. The study presented in Publication I was made using fracture mechanics to model the behaviour of the internal cracks combined with the finite element method to homogenize the microcrack responses over the continuous domain.

Overview

As discussed in Chapter 2.1, typical quasi-brittle materials such as concrete and rock contain numerous initial cracks that grow and adjoin under sufficient mechanical loading. The cracks affect the mechanical response of the material even before the crack growth, as demonstrated in Publication I.

The objective of Publication I was to develop and implement a method that can capture the effects of microcracking in a solid material, particularly in terms of the crack interaction, loss of stiffness and susceptibility to fracture. The specifics of the developed method were discussed in Chapter 3.1. The method was applied to crack arrays which were representative of manufacturing defects in additive manufacturing (AM) materials where the incomplete solidification during manufacturing may leave porosity and volumetric and planar defects in the

material (Herzog et al., 2016). The layer-by-layer AM production process tends to leave crack-like defects along the build layers if the heat input is insufficient, but also random patterns have been observed to occur, particularly if too much power is applied in the manufacturing (Sanaei et al., 2019).

The clearest effect that the microcracks have on a material is the reduced strength. For brittle and quasi-brittle materials, the reduction occurs in the static tensile and compressive strength whereas more ductile materials may tolerate the microcracking under static loading due to plastic dissipation but microcracks are known to reduce the fatigue strength of ductile metals (Murakami, 2019). Besides affecting the strength, internal cracks can cause an anisotropic stiffness of the material, as discussed in Chapter 2.2.1, or affect the location of initiation or the growth path of the macroscale failure. Publication I focused on these aspects by evaluating the microcrack interactions, increased susceptibility to fracture and the change in the apparent stiffness and anisotropy of the defectfull material, prior to crack growth.

Application

The applicability of the method was demonstrated with simulations of simple materials testing specimen geometries: unit cells under uniform tension and shear, four-point bending specimens and round and tensile tests on sharp-notched specimens. The behaviour of different oriented and random crack patterns were studied in each case. The random arrays tend to average the interaction effects out while the oriented defect patterns, typical to AM materials, produce the highest interaction or shielding effects. Figure 21 shows a horizontally oriented crack distribution in a notched tensile specimen and an example of how the interaction of the cracks deviates the crack face loading from the constant far-field tractions. Both amplifying and shielding effects are seen in the crack face traction distributions in the figure.

Results

The developed method captures the crack interaction effects in the structural scale, which is an outcome that could not be obtained using the normal structural stress analysis and fracture mechanics approaches separately. The finite element modelling of the structural geometry provided the correct stress states for the cracks in the material, while the opening displacements of the cracks contributed to the continuum softening of the material, which had a feedback type effect on the stress solution. Moreover, the crack closure caused an anisotropic effect on the material response on the structural scale. A particularly interesting observation of the interaction behaviour was the competition between the interaction amplification and shielding effects, caused by the collinear and stacked cracks, respectively. The dense crack arrays typically caused second-order mixed-mode effects, where the shear stress fields raised by the cracks induced considerable shear deformation on the adjacent cracks. Modelling the true response of a component containing a large number of defects requires that the interaction of the cracks is considered accurately and that the effects are propagated onwards to the finite element solution. Such an assessment had not been reported in the literature previously.

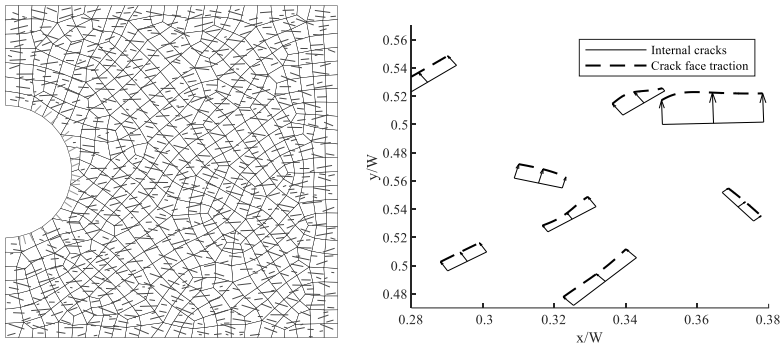

Figure 21. An oriented array of internal cracks in a round-notched specimen with surface cracks on the notch (left) and an example of the traction distributions acting on the internal cracks after the interaction calculations (right). Figure adapted from Publication I.

Figure 22 shows the typical results obtained in the calculations of Publication I. The left-hand side colour contour shows the total strain in the direction of the applied tensile load, normalized with the elastic strains in the matrix. The crack interaction system is overlaid with the black lines. The darkest red colours indicate regions where the surrounding microcracks degrade the local stiffness the most and lead to the highest total strains. The right-hand side plot shows the stress intensity factors of each crack in the system, normalized with the highest SIF before the interaction. The overall statistics of the stiffness degradation and the SIF amplification are shown below the figures.

The first example case in Publication I, a rectangular specimen under uniform loading, also served as the calibration and validation for the method. The results for this case showed a behaviour which was in agreement with the analytical solution of infinite crack arrays, both in terms of stiffness and SIF amplification. The influence radius of the RVE homogenization (see Chapter 3.1) was calibrated to be r_0=0.3 mm by studying structured crack arrays with the method and comparing the SIF and stiffness results with the analytical solutions. A radius which was too small led to spatially oscillating differences in the elements' stiffness degradation and the cracks' responses, while a radius which was too large led to the loss of the spatial resolution in the finite element solution similar to the result obtained with a coarse element mesh.

The oriented crack arrays, such as the one shown in Figure 22a, produced the highest amplification and shielding effects both in the SIF values and in the stiffness degradation. The interaction between the cracks in the case of Figure 22a increased the maximum SIF in the system by 17.3 %, which directly correlates with the increased susceptibility to fracture onset. The nonlinear crack interaction solution caused crack closure in some of the cracks, which is seen in the zero SIFs in the SIF plot of Figure 22a. Without interactions, the dense array of cracks would reduce the stiffness of the specimen by 38.7 %, but the closure of some of the cracks increased the stiffness of the specimen by 20.7 percentage points. As seen in the other results of the rectangular specimen geometry presented in Publication I, the interaction effects in the random arrays cancelled each other out, which is consistent with previous reports (Kachanov, 1993). The

crack closure and friction effects included in the calculations caused the shear-loaded specimens to behave more stiffly than predicted analytically.

The bending example (Figures 3 and 11 of Publication I) showed that the structured crack systems can produce a notably anisotropic response as the cracks located on the compressed side closed, mitigating their effect on the material stiffness, while the cracks under tension opened. This moved the neutral axis towards the compressed side. The response was mirrored as the load direction was reversed.

In the round-notched specimen, a surface crack shielding effect due to interaction was observed (Figure 22b). Without the interactions, the cracks opening to the round notch surface would experience the highest opening. However, when accounting for the crack interaction, these parallel cracks shielded each other. This caused the internal cracks next to the edge cracks to become the most critical in the system. Such a result could not be obtained without the combination of the finite element method to compute the stress hotspots and the crack interaction calculations to obtain the crack shielding effects. Quantified by the SIF values, the interaction reduces the susceptibility to fracture by 19.9 %.

Discussion

The implemented method was able to reproduce microcrack system behaviour and continuum softening effects in line with the previously reported results for cracked solids (Kachanov, 1993). The SIF amplification results for the simple periodic arrays agreed with the corresponding analytical solutions and the stiffness degradation calculated for the random crack arrays corresponded to the predictions made analytically without the interaction effects. Further, in the more complex example cases, the method was able to capture the non-uniform stiffness degradation and interaction effects dependent on the structural stress gradients. The fracture process zone-type effects were also observed in the simulations. The scope of the work was limited to the pre-growth period in the full failure process. The process continues with the growth and coalescence of the cracks, which is addressed in the next section and in Publication II, where the compressive failure induced by the internal cracks in the material is studied.

Publication I showed that considering the crack interaction is required to capture the variations in the crack face tractions, which is essential in obtaining the correct stress intensity factors and crack opening displacements. The interaction effects can be neglected in the case of truly random crack arrays if the interest is only in the stiffness of the material and not the increased susceptibility to failure. Amplification or shielding effects are typical in oriented crack arrays and considerable anisotropy can be introduced, if some of the microcracks are closed by compressive stresses, which makes the anisotropy a non-local phenomenon. These features are inherent to the pre-failure behaviour of any material with multiple non-negligible internal flaws and need to be considered when formulating constitutive models of the local stress-strain response of the material.

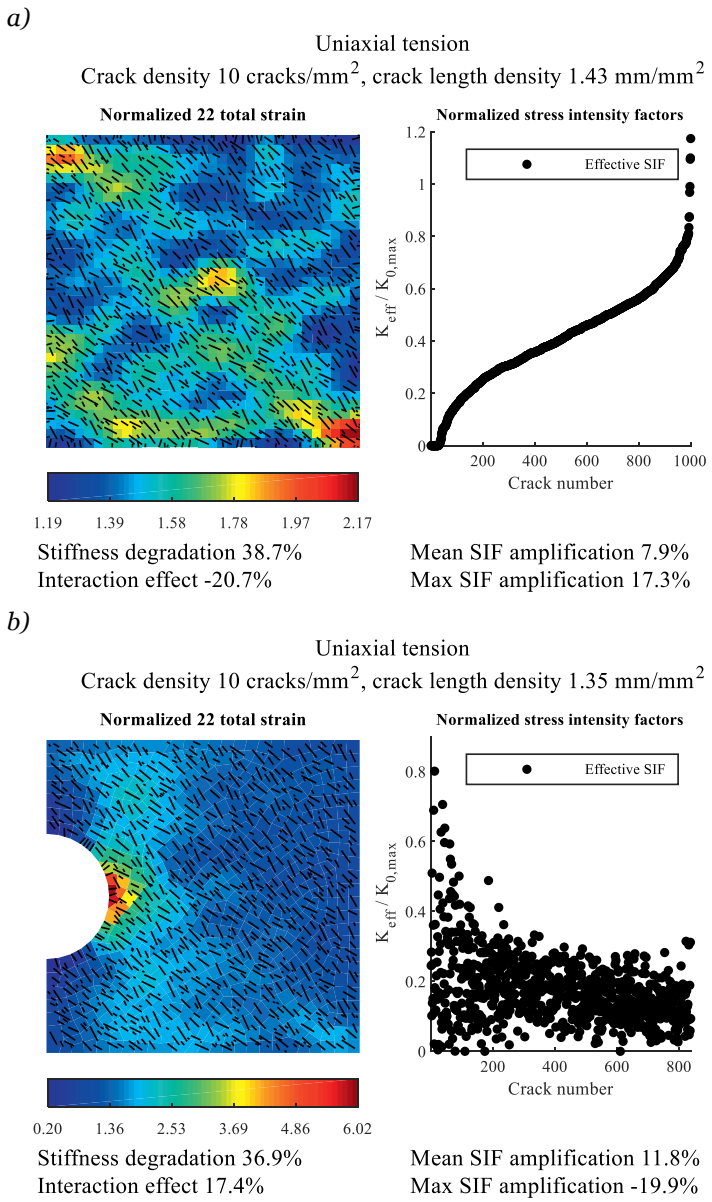

Figure 22. Macroscopic strain fields and stress intensity factor results of the internal cracks calculated for uniaxial tensile specimens (a) and round-notched tensile specimens (b). The stress intensity factors are normalized with the highest SIF not considering the interactions. Figure adapted from Publication I.

The examples considered crack patterns caused by an additive manufacturing process assuming an elastic matrix for the material. The process typically causes patterns aligned with the build direction. The initial defects or suitable initiation sites in inhomogeneous materials such as concrete, rock and ice are controlled by the internal structure of the material, which can lead to aligned crack patterns due to the grain structure, for example. Although performed at a different

scale, the calculation cases can be considered to be indicative of the defect interaction effects in ice, where the cracks tend to initiate at the grain boundaries (Schulson and Duval, 2009). Cole (1986) reports the crack spacing to grain size ratio of approximately 0.5 for polycrystalline ice loaded in creep conditions, depending on the amount of axial strain. Schulson and Duval (2009) report that defect densities of ~0.3 mm/mm^2 could be introduced in columnar ice by prestraining but the defects had no effect on the compressive strength. Publication I of this work studied crack length to spacing ratios of the same magnitude, i.e. above 0.5, and defect densities above 0.7 mm/mm^2. A regular 2-D hexagonal pattern containing cracks along one parallel side between all hexagons results in a defect density of approximately 0.6 mm/mm^2. Therefore, the calculations in Publication I approximate the highest internal crack interaction effects expected to occur in ice, which depend on the length and spacing of the closely-packed cracks, but overestimate the overall defect density as the defects would need to be initiated at each grain boundary, which, in turn, affects the total compliance of the material.

The work summarized in this chapter addresses the combined effects of internal cracks, and how to represent the discrete internal flaws as continuum damage effects. The numerical representation of the quasi-brittle failure process, dissected in Figure 2, continues with the growth and coalescence of the internal flaws in the next chapter.

4.2 Crack coalescence and macroscopic fracture

Overview

This section presents the modelling results of microcrack growth and coalescence under confined compression. Publication II models the compressive failure of a material containing periodic arrays of initial cracks, which propagate by the wing crack mechanism as discussed in Chapter 3.2. These studies belong to the second phase of the failure process of quasi-brittle materials dissected in Figure 2. This phase includes the growth and coalescence of the internal cracks up to the point of the first macroscopic fracture.

Assumptions

The main focus of the work presented in Publication II was to evaluate the interaction behaviour of 3-D wing crack systems that propagate driven by the external compression. The corresponding 2-D systems were solved for comparison. The studied crack arrays shown in Figure 23 are regular periodic systems of penny-shaped main cracks that grow via the wing crack mechanism, which is shown in Figure 15. According to the idealization of the wing cracks, the cracks were represented with planar cracks (Chapter 3.2). As shown in Publication II and summarized below, the interaction effects play a key role in causing the unstable failure. The most critical crack array configurations leading to the smallest compressive strength were sought in the study. Therefore, the interaction effects between the cracks in the critical geometrical configurations were always amplifying instead of shielding.

All initial cracks in the periodic arrays were assumed to be co-planar, but typically not aligned with the plane adjoining the crack centre points. The most critical orientation of the cracks was sought in the calculations. The behaviour of periodic, i.e. infinite, arrays were studied. However, the infinite arrays were represented with a finite number of cracks, namely a system of 11×11 cracks, which was determined to provide a converged solution for the middlemost cracks (see Table 2 of Publication II).

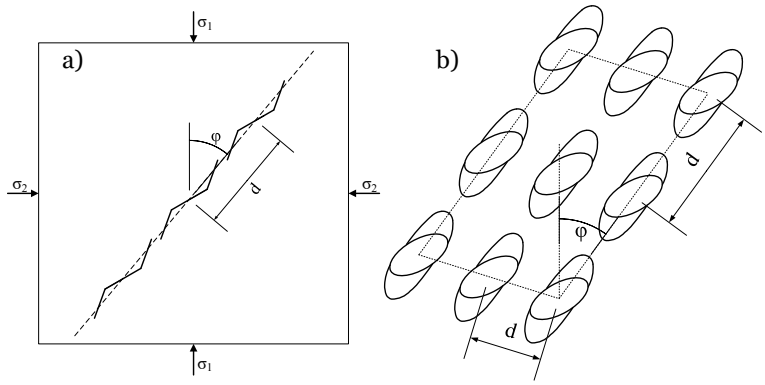

Figure 23. The studied arrays of internal wing cracks in 2-D (a) and 3-D (b). Figure adapted from Publication II.

The orientations of the crack system plane and the initial cracks were considered as fixed initial conditions in the calculations and the crack propagation direction was calculated by maximizing the Mode I stress intensity factor. Based on the most susceptible propagation direction, the magnitude of the external load was determined based on the condition that the maximum stress intensity factor obtained within the crack array was equal to the specified fracture toughness. After solving the critical external load, a small growth increment to the cracks was applied and the new system was solved identically.

To determine whether suitably oriented crack arrays can produce a shear-like failure in a 3-D setting, two kinds of crack systems were studied: 1) a system with large cracks far apart and 2) a system with small closely-spaced cracks. Without lateral confinement, system 1) is known to be more brittle than system 2) both in 3-D and 2-D. With lateral confinement, the crack growth in both systems would be arrested if it was not for the interactions.

Results

The results of Publication II showed that the interaction can cause the crack system 2) to produce a macroscopic failure both in 3-D and in 2-D, while the system 1) remains not critical. The possibility of an unstable macroscopic failure was evaluated from graphs of the critical external load plotted against the crack length, as shown in Figure 24.

The study assumed load control and the instability was assumed to occur once the magnitude of the external load yielding the critical stress intensity factor started to decrease with the increasing crack length. A plot of the critical external load of the calculation case where the crack array plane orientation is 20°

with respect to the maximum compressive load is shown in Figure 24, both with and without lateral confining pressure and as a function of crack plane friction. The figure shows that the larger cracks can grow both in 2-D and 3-D when there is no confinement (subfigures a and e), but the lateral pressure arrests the cracks (3-D, subfigure b) or causes the propagation to remain stable (2-D, subfigure f). The smaller, closely-spaced, cracks under confinement retain their ability to grow in 3-D (subfigure d), but they are not as unstable as in the 2-D setting (subfigure h). The smallest critical load levels are observed with small closely-spaced cracks under uniaxial loading (subfigures c and g). The crack growth paths and critical external loads are visualized in Figure 25. This is the main result of Publication II and it confirms the hypothesis that the interaction of the cracks can cause a shear-like failure in 3-D. Moreover, it was shown that the crack interaction system in a 3-D setting behaves in a manner not correctly predicted by 2-D models. The friction on the crack plane can effectively strengthen the material, as it limits the sliding of the crack faces, which would lead to the propagation of the initial cracks. The quantified interaction effects are seen in Figures 3-6 of Publication II.

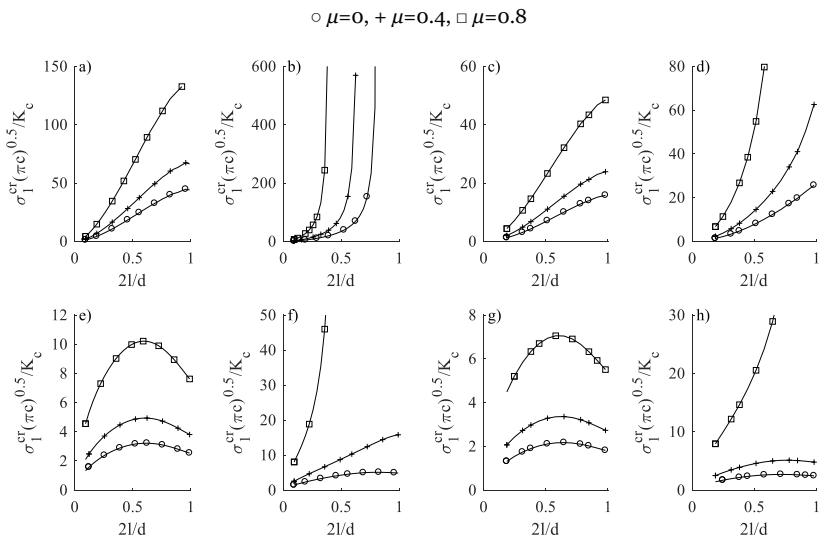

Case 1A. Large cracks far apart, no confinement.

Case 1B. Large cracks far apart, 5 % confinement.

Case 2A. Small cracks close to each other, no confinement.

Case 2B. Small cracks close to each other, 5 % confinement.

Figure 24. The normalized external load required to initiate a macroscopic fracture in the 3-D (a-d) and 2-D (e-h) crack arrays calculated with different crack face friction coefficient μ. Figure adapted from Publication II.

Discussion

A typical trend in the calculations of Publication II was that the interaction effects reduced the critical load magnitude, with this effect being stronger in 2-D than in 3-D. This is consistent with the conclusions by Kachanov (2003) and is primarily caused by the more rapid attenuation of the crack tip stress fields in 3-D than in 2-D.

The calculations confirmed the main hypothesis of Publication II: It was shown that a shear-like fracture, due to the interaction of the cracks, can occur in a 3-D setting. Under lateral confinement, the 2-D geometry resulted in an unstable fracture caused by the interaction, while a full crack coalescence in the 3-D setting required a constantly increasing external load. Without the interactions, the 3-D wing cracks would eventually be arrested. Horii and Nemat-Nasser (1985) reported the same behaviour in transparent 2-D resin samples. The confining pressure arrested the growth or larger isolated cracks, after which suitably oriented smaller, closely-spaced, cracks adjoined to produce a shear-like fault.

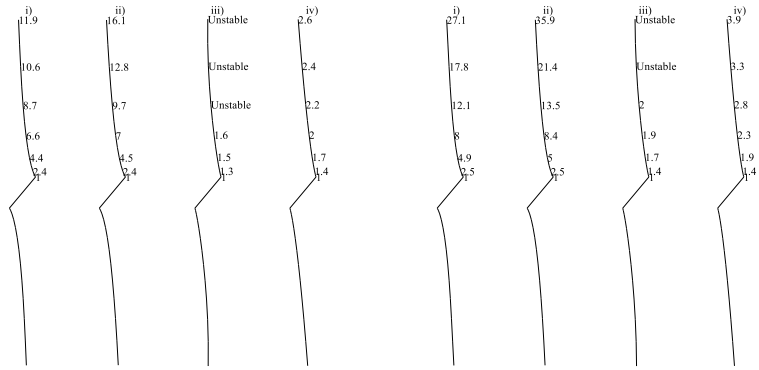

Case 2A. Small cracks close to each other, no confinement.

Case 2B. Small cracks close to each other, 5 % confinement.

Figure 25. Schematic scale drawings of the trajectory of a single crack in the 3-D crack interaction system (i), 3-D single crack case (ii), 2-D crack interaction system (iii) and 2-D single crack case (iv). The numbers denote the relative magnitude of the compressive load required to extend the crack before the final instability. The main compressive load is applied vertically. Figure adapted from Publication II.

In the calculations, the interaction affected the load magnitude required to cause crack propagation but not the propagation direction. The cracks constantly propagated towards the direction of the maximum applied external load, consistent with the experiments by Dyskin et al. (2003) and Y. P. Li et al. (2005).

It is important to consider the implications of the results for the modelling of the compressive failure process in the structural scale. The behaviour of the 2-D and 3-D models were clearly different and the 2-D model could be used to predict the 3-D failure behaviour. These findings question the typical engineering simplification, utilised also in Chapter 4.4, in which only a slice of the true 3-D geometry is modelled and the obtained results are scaled with the width of the structure to estimate the actual load magnitude.

This chapter addressed the phase of the quasi-brittle failure process (Figure 2), in which the internal cracks grow and adjoin to cause the first macroscale fracture in the material. The next phase of the quasi-brittle failure process, the discretization of the internal fractures within a finite element framework, is addressed in the next chapter.

4.3 Discretization of internal fractures

Overview

This section presents the modelling results obtained using the remeshing approach developed to discretize the internal damage originally presented in Publication III. These studies consider the third phase, the discretization of the internal fracture, of the numerical representation of the quasi-brittle failure process dissected in Figure 2.

As discussed in Chapter 2.2.4, in many cases it is desired that the damage predicted by continuum damage models could also be represented discretely. This requires techniques beyond constitutive models. Publication III presents a numerical finite element method compatible approach which was developed to transfer the internal damage predicted by a smeared crack material model into an explicit fracture represented by the free boundaries of the simulation model. The main objective of the paper was to propose, implement and test a local remeshing procedure suitable for discretizing damage in quasi-brittle materials. The details of the developed method were presented in Chapter 3.3. The approach was validated with the example simulation cases that are presented in this section.

Results

The approach was validated with two test cases, a Mode I splitting case and a Mode II shear crack propagation case, as visualized in Figure 26 and Figure 28. The first test case modelled the tensile splitting of a pre-cracked plate. Consistent with the direction of the applied load and induced maximum stress, the approach predicted vertical crack propagation until the crack extended near the opposite edge of the plate (Figure 26). The load-displacement relation shown in Figure 27 indicates very little mesh dependency, no visible disturbances caused by the remeshing and is in qualitative agreement with the reference results by Areias and Belytschko (2005). The utilized simplified damage model produced a more brittle post-peak response than in the reference results.

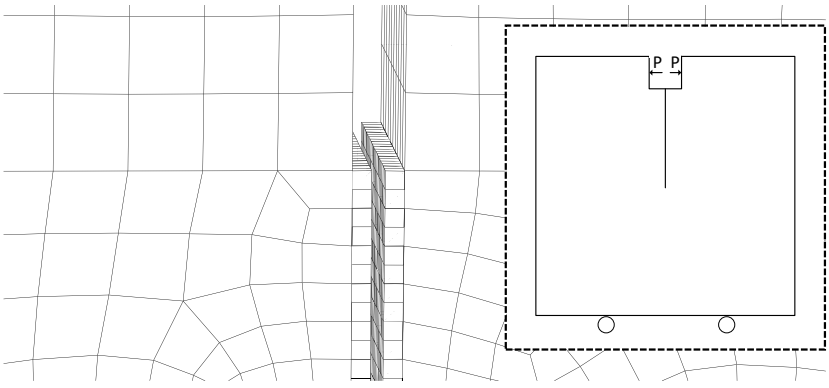

Figure 26. Mode I crack propagation from a notch in a pre-cracked plate calculated with the remeshing method. The elements along the pre-crack have been remeshed. Figure redrawn from Publication III.

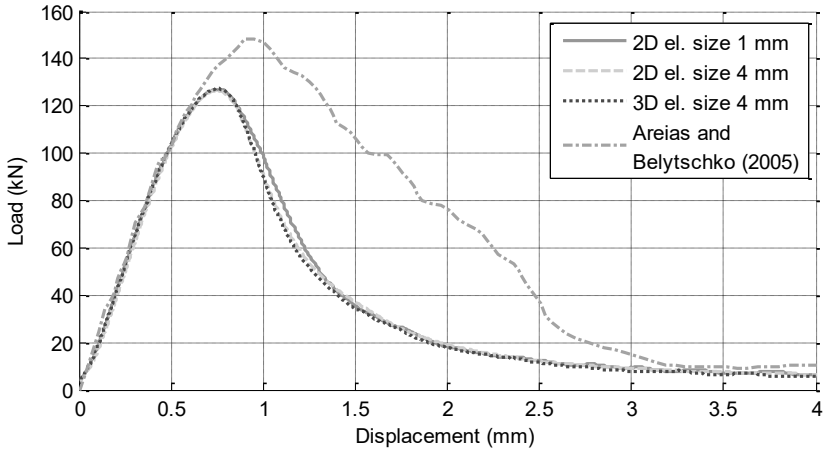

Figure 27. Load-crack mouth opening displacement curve for the pre-notched plate simulation calculated with different element sizes both with 2-D and 3-D models and a reference result from the literature. Figure adapted from Publication III.

The second test case shown in Figure 28 considered Mode II crack propagation in a double edge cracked plate subjected to shear loading. The cracks propagated from both of the side notches and avoided each other in a manner similar to the reference results by Jäger et al. (2009). Despite the simplified softening relation, the global load-displacement response shown in Figure 29 is in good agreement with the reference result. This case also includes an example of the crack interaction effects on the macroscale as the cracks tend to avoid each other during propagation.

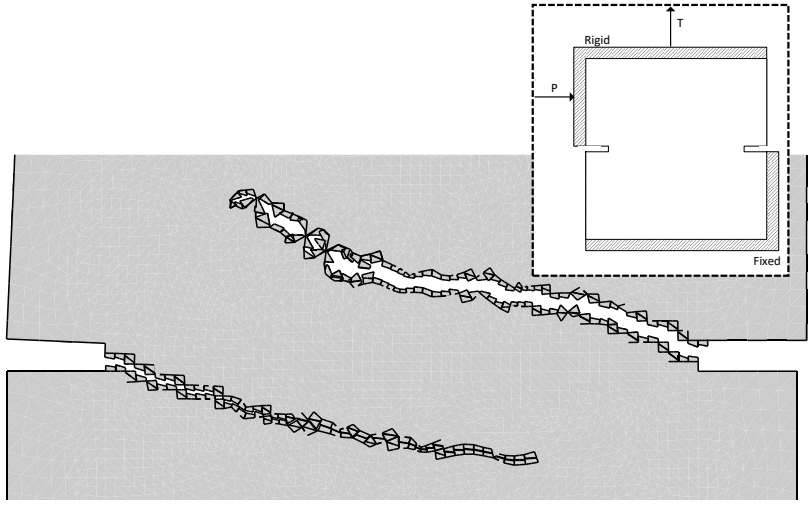

Figure 28. Mode II crack propagation in a double edge cracked plate calculated with the remeshing method. The displacements are magnified 100 times and only the newly created elements are shown. Figure redrawn from Publication III.

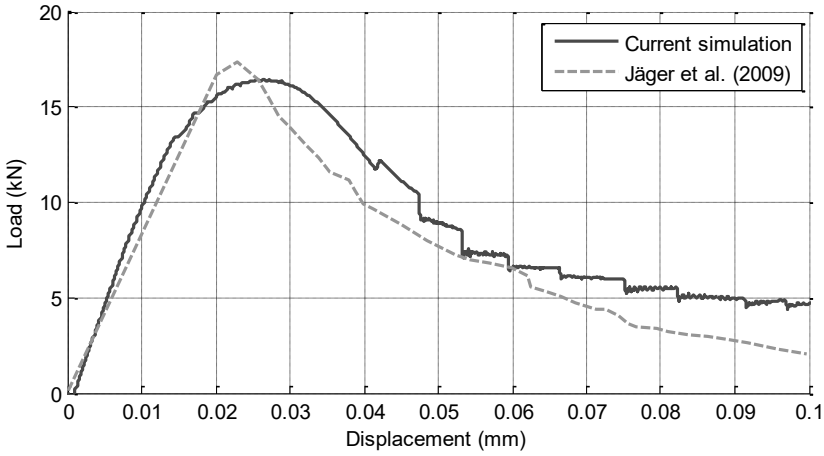

Figure 29. Load-vertical displacement relation double edge cracked plate simulation compared with a reference simulation from the literature. Figure adapted from Publication III.

Discussion

The developed approach performed well in the test cases included in Publication III and was able to predict the correct crack propagation paths. The applied material model controls the resulting load vs. displacement relations, but even the simplified model performed reasonably well. The test cases above did not include any significant crack face contact or fragmentation of the material. The feasibility of the method in such a case was qualitatively demonstrated with an ice sheet global bending failure simulation included at the end of Publication III. The example demonstrated qualitatively how the approach is able to produce some important aspects of the ice sheet bending failure process, namely fragmentation and cracking in tension. Other failure modes occurring during the crushing process are not included in the model at its current state, which limits the true applicability of the model as the only energy dissipation mechanism is through tensile cracking.

The presented examples modelled essentially 2-D crack propagation, although the implementation was made in a 3-D setting. Thus, the approach is, in principle, able to cope with variations in the fracture process along the third dimension and is sensitive to out-of-plane confinement. The results of Publication II (Chapter 4.2) indicated that such aspects are important to consider when predicting the growth paths and failure stresses of internal cracks.

The simplified softening model used in the work set limits on the direct applicability of the implementation, but the material model was considered of secondary importance and other, more sophisticated, damaging models can be employed without modifications to the simulation method. The primary focus is the remeshing method, which can be applied with any kind of damage model provided that the model predicts the complete and oriented softening in the material. The largest drawback in the implementation of the method were the limitations set by the commercial FE code Abaqus used in the calculations. The simulation model mesh could not be modified during the analysis as new ele-

ments could not be added into the calculation without interrupting the simulation. This required that the analysis was stopped for each remeshing, a new model definition file written, and the solution restarted. This limited the feasible number of remeshing rounds during one simulation. Therefore, additional developments of the approach to model discrete cracking were required to make the approach more compatible with the FE code Abaqus. The developments are presented in Publication IV and summarized in the next chapter.

This chapter presented an example of the methods needed to transform the internal continuum damage (i.e. microcracking) into discrete damage, which was identified as the third phase of the numerical quasi-brittle failure process in Figure 2. Other methods of this type were discussed in Chapter 2.2.4. The final phase of the process considers the continuous propagation of internal failures. An example of such behaviour is presented in the next chapter.

4.4 Propagation of discrete cracks and post-failure behaviour

Overview

The fourth phase of the numerical representation of the quasi-brittle failure process of Figure 2 includes the propagation of discrete fractures through the material and representation of the post-failure behaviour. The crushing of an ice sheet was studied as an example of a case where the propagation of multiple discrete fractures through the material and the subsequent fragmentation control how the failure continuously progresses. As presented in Chapter 3.4, the cohesive surface methodology was implemented for this purpose. The method utilized the fictitious crack model to predict the failures in the material and the finite element method and cohesive elements to discretize the failures. This section summarizes the ice sheet continuous crushing simulation results presented in Publication IV.

As discussed in Chapter 2.2.4, the modelling of a continuous failure process requires techniques beyond the traditional finite element method and a suitable constitutive model for the material in question. The aim of Publication IV was to develop and apply a technique for modelling the continuous crushing of an ice sheet against a vertical target. The laboratory ice block crushing experiments by Määttänen et al. (2011) were simulated in the work. The test setup is shown in Figure 30. The simulations tested and calibrated the approach outlined in Chapter 3.4 designed to capture the onset and propagation of the crushing failure and the fragmentation of the ice sheet, while keeping the separated fragments in the simulations. Besides the indentation failure process of the ice sheet, the simulations studied the pressure distribution the crushing induces on the vertical structure.

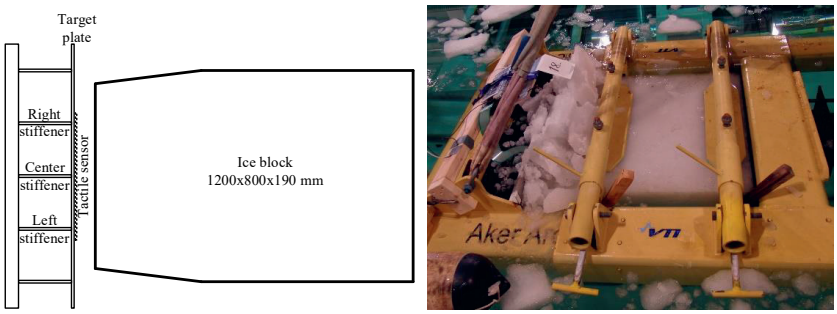

Figure 30. The configuration of the studied ice block crushing test and a photo taken after the crushing. The drawing is taken from Publication IV and the photo is from the test campaign by Määttänen et al. (2011).

Mechanically, ice-structure interaction is a complex process and can include various failure modes (Schulson and Duval, 2009). However, the ice sheet failed by crushing and fragmentation with the temperature and velocity in the studied crushing tests by Määttänen et al. (2011). Different aspects of the ice crushing failure process are discussed in Publication IV to outline the behaviour targeted in the simulations and more thoroughly by Jordaan (2001). Relevant to the context of this thesis is that the crushing is a continuous and repetitive fragmentation process. Predicting the fragmentation accurately and keeping the fragments active in the simulations are essential to correctly capture the progression of the failure process.

The simulations in Publication IV were performed by considering a thin slice in the middle of the ice sheet, assuming plane strain conditions. Planar finite element models consisting of triangular elements were utilized in the simulations. In the validation of the modelling approach, the simulations studied how different mesh densities and randomness in the mesh affected the failure process. Moreover, the effects of different softening relations were tested for the interface elements. An example of the simulation model for the ice sheet is shown in Figure 31. The densely meshed left end of the ice sheet contains bulk elements surrounded by the cohesive elements and the failure process is restricted within this region while the other end of the sheet provides the constant-velocity thrust and appropriate boundary conditions for the front part of the sheet. Gravity and buoyancy were included in the simulation to keep the separated fragments with the ice sheet body.

Results

Snapshots of the simulated failure process are shown in Figure 32. The figure, and the corresponding figures in Publication IV, demonstrate the applicability of the method. It can be seen how the separated fragments remain in the crushing region and affect the later failures, consistent with the experimental observations made in the test (Määttänen et al., 2011). In most of the analyses, the first failure separated one or two wedge-shaped fragments from the front of the ice sheet, after which smaller failures took place. The separated fragments remained near the front of the ice sheet and affected the later fractures. The frag-

ments separated from the bottom of the sheet typically flowed downwards, unstopped by the small buoyancy resistance, while the fragments separated from the top were held in the contact region by gravity. The separated fragments started to pile on top of the sheet towards the end of the simulation. The interface elements behind the crushing region remained intact indicating that the failure process was localized near the vertical structure without bending failures further from the contact zone.

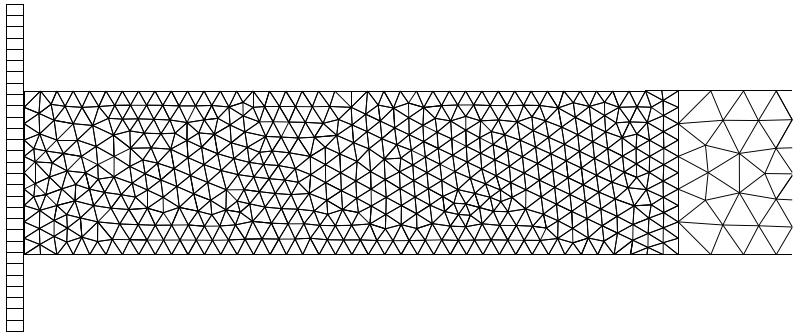

Figure 31. An example of the ice sheet mesh using cohesive surface methodology. The fracture process is captured in the densely meshed left-hand end. The cohesive elements are too thin to be visible between the solid elements. Figure redrawn from Publication IV.

The simulations with different mesh sizes showed similar characteristics with both small and large separating fragments and local contact areas much smaller than the ice sheet thickness. However, somewhat different failure patterns were observed, depending on the mesh size and the traction-separation law. The failure process was seemingly random such that the type and shape of the initial failure guided the process into a unique path making the simulation cases differ from each other. A similar observation has been also made experimentally (Jordaan, 2001).

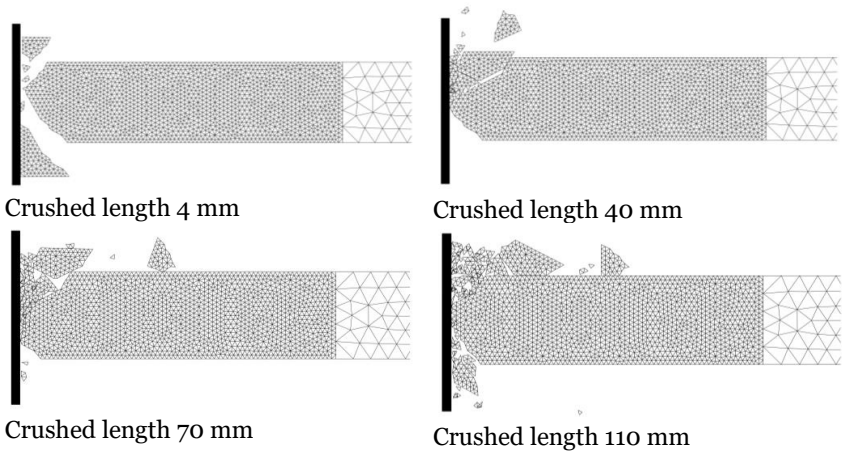

Figure 32. Example of the progression of the crushing failure process calculated with a dense simulation mesh. Figure redrawn from Publication IV.

Examples of the contact force records obtained in the simulations are shown in Figure 33 (left). Although the macroscopic appearance of the failure process varied in different cases, the contact force vs. time histories were similar for each mesh. The coarser meshes separated larger fragments, which led to higher force peaks and longer delays between the peaks whereas the densest mesh showed more noise-like contact forces with more frequent, but smaller, force peaks. A saw-tooth shape in the contact forces, particularly with the coarser meshes, can be observed, which is consistent with experimental observations (Jordaan, 2001; Määttänen et al., 2011). A comparison between the simulated contact force from one of the simulation cases and that measured experimentally from the centremost stiffener supporting the target structure is shown in Figure 33 (right).

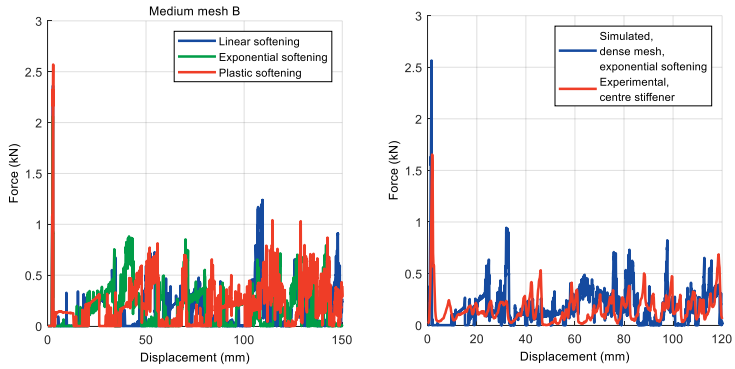

Figure 33. Left: Contact forces calculated with different softening models. Right: Comparison of the simulated contact force with the experimental measurement. Figure redrawn from Publication IV.

Being two-dimensional, the simulations showed pointwise contact at the ice-structure interface, which corresponds to a line-like contact in 3-D. The location of the contact point in the simulations varied during the failure process. Figure 34 shows the vertical location of the nodes experiencing contact during the simulation as a function of the ice sheet movement. The leftmost vertical line of dots in the figure is the initial uniform contact and the subsequent points correspond to the hot-spot type of contact occurring after the initial failure. The softening models in the graph titles in Figure 34 are those shown in Figure 20.

Discussion

The work in Publication IV showed that the applied methodology can be applied to simulate the ice crushing process occurring under brittle conditions. A reference test denoted as brittle by Määttänen et al. (2001) was selected. The indentation crushing of ice is typically classified between ductile and brittle based on the indentation velocity (Jordaan, 2001). At the material level, the controlling factors are temperature, strain rate and confinement pressure. An indentation classified generally as brittle may experience locally ductile behaviour, particularly at the high-pressure contact zone. Such aspects are not captured by the current implementation. Failures occurring away from the contact

zone are expected to remain brittle and are thus within the applicability limits of the methodology.

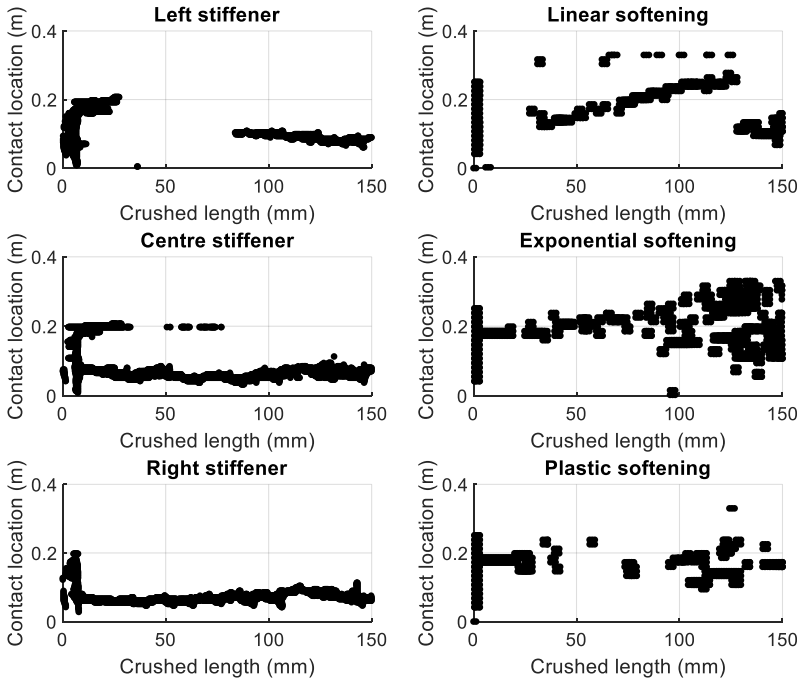

Figure 34. Measured (left) and simulated (right) evolution of the contact location as a function of crushing displacement. The simulation results with all three softening models are shown. Figure redrawn with the original data used in Publication IV.

The method predicted similar ice crushing behaviour to that observed in the experiments, in terms of the fragmentation process, type of contact and the trends and magnitudes of the contact forces. The contact forces and contact locations demonstrate the chaotic nature of the simulated crushing process. For example, a change in the shape of the softening function steers the process onto a completely different path. The results do not indicate that any of the studied softening relations is superior to the other models. The simulations confirmed that the modelling of fragmentation and especially the interaction of the fragments with the intact body are required to capture the progression of the failure process.

The cohesive surface approach adopted for the simulations (Chapter 3.4) naturally resulted in the crack formation, propagation and branching as the cohesive elements fail due to the external load and separated fragments from the initially intact material. The crack propagation paths were, of course, limited by the topology of the mesh. While the constitutive behaviour of the interface elements is isotropic, the varying orientations of the interface elements produce an anisotropic failure behaviour in the macroscale. The selected simulation method was able to produce the macrocracking leading to the fragmentation,

but not the microcracking that precedes the macrocracking as the size scale of the microcracking is well below the discretization scale in the finite element mesh. Moreover, the traditional continuum damage models (see Chapter 2.2.2), or models formulated based on the representation of the microcracks in the material (as in Chapters 3.1 and 3.2) would be better suited to capture the microscale behaviour before the fractures on the structural scale. The developments presented in Publication III discussed previously were initiated to apply the method for an analysis similar to the one performed here. As discussed in Chapter 4.3, it became evident during the work that the strength of that method was in modelling the propagation paths of a limited number of fractures accurately and capturing a continuous fragmentation process is unfeasible. The method applied in Publication IV is better suited for this task, as demonstrated here. The work highlights that the representation of the fragmentation kinematics allows capturing a large part of the brittle crushing failure process and the methodology leaves room for improvements in the aspects not currently considered.

Besides the simplified constitutive model, the method is not currently mature enough to be used in the accurate prediction of the ice crushing loads, even in the brittle regime. The simulations considered a slice of the material uniformly confined in the out-of-plane direction. In Publication IV, the next logical step was identified to be the application of the method in a 3-D setting as the experiments indicated that the failure process does not behave uniformly along the contact line (Määttänen et al., 2011), which causes variations in the confinement in the third direction both along the crushing front and away from it as the crushing progresses. Moreover, the results obtained in Publication II and summarized in Chapter 4.2 highlight the importance of considering true 3-D geometries instead of their 2-D idealisations when modelling failure processes with a triaxiality dependence and a variation in the out-of-plane direction. This extension was, however, deemed too expensive due to the vast increase in the computational effort required. The computing power has increased since and such efforts have been recently published (Wang et al., 2018, 2019), although on a larger scale with a lower spatial resolution of the fracture paths inside the material. A 3-D simulation of the local crushing and continuous fragmentation process has not been published yet.

These developments are a part of the fourth and final phase of the numerical quasi-brittle failure process in Figure 2. The phase follows the initiation of discrete fractures and is focused on the growth and propagation of multiple cracks and the fragmentation process of the material.

5. Concluding remarks

The numerical modelling of quasi-brittle failure is an active research topic as the normal structural analysis methods often fall short when the changes in the material stiffness or structural topology due to the fracturing need to be captured. The motivation to undertake this work was that there were no ready-to-use tools available to model the full failure progression, starting from the first microcracking and ending with the large-scale propagation of multiple fractures in the material. For engineering applications, it is important that the methods are compatible with commercial FE codes to take the full advantage of the other capabilities provided by the software. To provide such simulation tools, the failure process of quasi-brittle materials was divided into separate phases and each phase was addressed individually. The four phases shown in Figure 2 are: (1) the behaviour and softening effects of microcracks in the material, 2) the growth and coalescence of the microcracks into the first macroscale failure, 3) numerical discretization of the internal damage into an explicit representation of the fracture and 4) the propagation of the macroscale cracking and post-failure behaviour. The developments made in the simulation methods are summarized in Chapter 3, while the new results obtained using the methods are presented in Chapter 4. The methods and results are presented in the accompanying publications in more detail. The main results and new findings made in this thesis are summarized below.

The methods developed in this work include:

- In Publication I, a novel method for predicting the crack interaction effects, both on local and global scales, was developed and validated using analytical test cases. The method couples the local behaviour of the microcracks with the global finite element solution of the component response.
- In Publication II, a 3-D expansion of a fracture mechanics approach to modelling microcrack growth and coalescence in confined compression was presented. The method combines wing-crack kinematics and crack interaction calculations to model how arrays of pre-existing penny shaped cracks propagate and connect to cause a compression failure. The 2-D counterpart of the method yielded results in agreement with the literature, providing validation to the approach.

- In Publication III, a novel remeshing method was developed, bridging the gap between the internal material point damage and explicit crack representation. The method implemented in the FE software Abaqus discretizes the internal fractures predicted by a continuum model into free surfaces of the element mesh.
- In Publication IV, a cohesive surface methodology was implemented in Abaqus FE software. The implementation which was able to capture local crushing and subsequent fragmentation of quasi-brittle materials in was the first of its kind.

The main results obtained with the developed methods are:

- The method developed in Publication I quantified the microcrack shielding and amplification effects under the structural stress gradients. Such an assessment had not been reported previously. Additionally, the surface crack shielding effects were shown to be strong enough to cause the surface cracks may be less prone to fracture than the adjacent internal cracks. The results emphasize why the interaction of the internal cracks needs to be considered as it has an effect both on the stiffness and on the susceptibility to failure of inhomogeneous materials.
- As a novel result, the method developed to model fracture under confined compression in Publication II showed that a shear-like failure due to the coalescence of adjacent cracks is possible also in a 3-D setting, but not with such an instability as in a 2-D geometry. It was shown that the interaction of the internal cracks contributes towards a failure mode observed as shear macroscopically. The stress amplification effect by the crack interaction was found to overcome the crack arresting effect by the lateral confinement.
- The remeshing method developed in Publication III was successfully applied and validated to model the discrete crack propagation along arbitrary paths. The accurate representation of the crack propagation paths of several cracks in the material and their interaction effects were demonstrated with the method.
- The capabilities of the cohesive surface approach presented in Publication IV were successfully validated by simulations of an ice sheet local crushing and fragmentation process. The method predicted fragmentation behaviour which was similar to the reference experiments and the trends and magnitudes of the simulated contact forces agreed with the experimental measurements.

An important and common feature identified in the developments and the cases studied in this work is the interaction of cracks, and particularly the effect of interaction on the early stages of the failure of quasi-brittle materials. The interaction can trigger the fracture with a considerably lower external load than that sustainable by a material with isolated flaws, or it can produce shielding,

which increases the apparent resistance of the material. Thus, the accurate modelling of fracturing of quasi-brittle materials requires that the interaction of the cracks is taken into account on several different scales, from the first small microcracks to the resulting macroscale cracking.

All methods developed in this work consider brittle or quasi-brittle fracture, where the deformation occurs by the growth and coalescence of the internal cracks in the material, first in the microscale and then in the macroscale. The initial focus of the developments was on the performance of the techniques from a numerical point of view. The example calculations and the applied material models and parameters are not be the best possible models for the studied scenarios. A number of limitations are present in the methods, particularly in the captured deformation mechanisms. Some of the limitations can be overcome by more detailed constitutive modelling and some require extensions to the developed numerical modelling approaches. However, the results demonstrate the feasibility of the methods and the accompanying discussion suggests ways of future improvement for each method.

Developing the methods required the utilization of different aspects of continuum mechanics, fracture mechanics and numerical approaches. Fracture mechanics formed the basis of the description of the microcrack response, continuum mechanics and constitutive models averaged the microcracking into the homogenized material response and the numerical techniques such as remeshing and cohesive elements provided the means to capture the progression of the failure. The developed methods have advanced the field of numerical fracture mechanics and provided new information of the failure process of quasi-brittle materials. The approaches modelling the microcracking were shown to be compatible with the normal material modelling framework of common FE software. Concerning the discrete cracking, the cohesive and other types of softening models can be combined with the developed numerical techniques to represent the macroscale damage such that the continuous failure process is captured using the traditional FE codes.

The ever-increasing computational power makes previously unfeasible techniques to model the fracturing of materials available for everyday use and new techniques are being continuously proposed. The research outlined in this thesis has contributed to this field by developing novel approaches suited for different phases of the failure process of quasi-brittle materials. The methods have been demonstrated to be applicable in cases relevant to the engineering community. The increase of computational power also allows the utilization of the developed techniques in true 3-D cases. While the developed methods are not restricted to 2-D, the applications in this work mostly considered planar geometries due to the computational capacity available at the time.

The methods were mostly developed and applied independently from each other. A logical next step in the research is to combine the efforts into a single methodology which would be able to capture the full failure process, starting from the initiation and growth of the microcracking and ending with the continuous crushing and fragmentation of the material, all within the same analysis.

Acknowledgements

The publications included in this work were prepared in the projects STRUTSI and DICE which were funded by industry, TEKES - the Finnish Funding Agency for Technology and Innovation, the Academy of Finland and the VTT Technical Research Centre of Finland. Research supporting the topics of this thesis was also performed in the Finnish Nuclear Power Plant Safety Research Programmes SAFIR2018 and SAFIR2022. The final preparation of the dissertation manuscript was funded by the VTT Technical Research Centre of Finland.

References

Abaqus (2017). Abaqus 6.17 Documentation.

Anderson, T.L. (2017). Fracture Mechanics, 4th ed. CRC Press, Boca Raton. https://doi.org/10.1201/9781315370293

Areias, P.M.A.A., Belytschko, T. (2005). Analysis of three-dimensional crack initiation and propagation using the extended finite element method. Int. J. Numer. Methods Eng. 63, 760–788. https://doi.org/10.1002/nme.1305

Ashby, M.F., Sammis, C.G. (1990). The damage mechanics of brittle solids in compression. Pure Appl. Geophys. PAGEOPH 133, 489–521. https://doi.org/10.1007/BF00878002

Atkinson, B.K. (1987). Fracture Mechanics of Rock, Fracture Mechanics of Rock. Elsevier. https://doi.org/10.1016/C2009-0-21691-6

Basista, M., Gross, D. (1998). The sliding crack model of brittle deformation: An internal variable approach. Int. J. Solids Struct. 35, 487–509. https://doi.org/10.1016/S0020-7683(97)00031-0

Basista, M., Gross, D. (2000). A Note on Crack Interactions Under Compression. Int. J. Fract. https://doi.org/10.1023/A:1007644608705

Bažant, Z.P. (1986). Mechanics of distributed cracking. Appl. Mech. Rev. https://doi.org/10.1115/1.3143724

Bažant, Z.P. (1991). Why continuum damage is nonlocal: Micromechanics arguments. J. Eng. Mech. https://doi.org/10.1061/(ASCE)0733-9399(1991)117:5(1070)

Bažant, Z.P. (2001). Concrete fracture models: Testing and practice. Eng. Fract. Mech. https://doi.org/10.1016/S0013-7944(01)00084-4

Bažant, Z.P. (2004). Scaling theory for quasibrittle structural failure. Proc. Natl. Acad. Sci. 101, 13400–13407. https://doi.org/10.1073/pnas.0404096101

Bažant, Z.P. (2005). Scaling of Structural Strength. https://doi.org/10.1016/B978-0-7506-6849-1.X5000-7

Bažant, Z.P., Caner, C., Carol, I., Adley, M.D., Akers, S.A. (2000). Microplane Model M4 for Concrete. I: Formulation With Work-Conjugate Deviatoric Stress. J. Eng. Mech. 126, 944–953. https://doi.org/10.1061/(ASCE)0733-9399(2000)126:9(944)

Bažant, Z.P., Jirásek, M. (2003). Nonlocal Integral Formulations of Plasticity and Damage: Survey of Progress, in: Perspectives in Civil Engineering: Commemorating the 150th Anniversary of the American Society of Civil Engineers.

Bažant, Z.P., Oh, B. (1983). Crack band theory of concrete. Mater. Struct. https://doi.org/10.1007/BF02486267

Bažant, Z.P., Planas, J. (1998). Fracture and Size Effect in Concrete and Other Quasibrittle Materials, 1st ed. Routledge, New York. https://doi.org/10.1201/9780203756799

Bažant, Z.P., Xiang, Y. (1997). Size effect in compression fracture: Splitting crack band propagation. J. Eng. Mech. https://doi.org/10.1061/(ASCE)0733-9399(1997)123:2(162)

Bobet, A., Einstein, H.H. (1998). Fracture coalescence in rock-type materials under uniaxial and biaxial compression. Int. J. Rock Mech. Min. Sci. https://doi.org/10.1016/S0148-9062(98)00005-9

Bremberg, D., Dhondt, G. (2009). Automatic 3-D crack propagation calculations: A pure hexahedral element approach versus a combined element approach, in: International Journal of Fracture. https://doi.org/10.1007/s10704-009-9313-z

Brooks, Z. (2013). Fracture process zone: Microstructure and nanomechanics in quasi-brittle materials. Doctoral Thesis. Massachusetts Institute of Technology.

Camacho, G.T., Ortiz, M. (1996). Computational modelling of impact damage in brittle materials. Int. J. Solids Struct. 33, 2899–2938. https://doi.org/10.1016/0020-

7683(95)00255-3
Carloni, C., Cusatis, G., Salviato, M., Le, J.L., Hoover, C.G., Bažant, Z.P. (2019). Critical comparison of the boundary effect model with cohesive crack model and size effect law. Eng. Fract. Mech. https://doi.org/10.1016/j.engfracmech.2019.04.036
Červenka, J., Papanikolaou, V.K. (2008). Three dimensional combined fracture-plastic material model for concrete. Int. J. Plast. https://doi.org/10.1016/j.ijplas.2008.01.004
Chaboche, J.L. (1988). Continuum damage mechanics: Part I-general concepts. J. Appl. Mech. Trans. ASME. https://doi.org/10.1115/1.3173661
Cole, D.M. (1986). Effect of grain size on the internal fracturing of polycrystalline ice, CRREL report 86-5.
Courtin, S., Gardin, C., Bézine, G., Hamouda, H.B.H. (2005). Advantages of the J-integral approach for calculating stress intensity factors when using the commercial finite element software ABAQUS. Eng. Fract. Mech. 72, 2174–2185. https://doi.org/10.1016/j.engfracmech.2005.02.003
Crouch, S.L. (1976). Solution of plane elasticity problems by the displacement discontinuity method. I. Infinite body solution. Int. J. Numer. Methods Eng. https://doi.org/10.1002/nme.1620100206
De Borst, R. (2001). Fracture in quasi-brittle materials: A review of continuum damage-based approaches. Eng. Fract. Mech. https://doi.org/10.1016/S0013-7944(01)00082-0
Dempsey, J.P., Cole, D.M., Wang, S. (2018). Tensile fracture of a single crack in first-year sea ice. Philos. Trans. R. Soc. A Math. Phys. Eng. Sci. https://doi.org/10.1098/rsta.2017.0346
Dempsey, J.P., Xie, Y., Adamson, R.M., Farmer, D.M. (2012). Fracture of a ridged multi-year Arctic sea ice floe. Cold Reg. Sci. Technol. https://doi.org/10.1016/j.coldregions.2011.09.012
Derradji-Aouat, A.D. (2003). Multi-surface failure criterion for saline ice in the brittle regime. Cold Reg. Sci. Technol. https://doi.org/10.1016/S0165-232X(02)00093-9
Dragon, A. (2002). Continuum damage mechanics applied to quasi-brittle materials, in: Allix, O., Hild, F. (Eds.), Continuum Damage Mechanics of Materials and Structures. Elsevier Science Ltd, pp. 165–203.
Dyskin, A. V, Germanovich, L.N., Ustinov, K.B. (1999). A 3-D model of wing crack growth and interaction. Eng. Fract. Mech. 63, 81–110. https://doi.org/10.1016/S0013-7944(96)00115-4
Dyskin, A. V., Sahouryeh, E., Jewell, R.J., Joer, H., Ustinov, K.B. (2003). Influence of shape and locations of initial 3-D cracks on their growth in uniaxial compression. Eng. Fract. Mech. 70, 2115–2136. https://doi.org/10.1016/S0013-7944(02)00240-0
Elices, M., Guinea, G.V., Gómez, J., Planas, J. (2002). The cohesive zone model: advantages, limitations and challenges. Eng. Fract. Mech. 69, 137–163. https://doi.org/10.1016/S0013-7944(01)00083-2
Fakhimi, A., Tarokh, A. (2013). Process zone and size effect in fracture testing of rock. Int. J. Rock Mech. Min. Sci. https://doi.org/10.1016/j.ijrmms.2012.12.044
Gagnon, R.E. (2011). A numerical model of ice crushing using a foam analogue. Cold Reg. Sci. Technol. https://doi.org/10.1016/j.coldregions.2010.11.004
Germanovich, L.N., Dyskin, A. V. (2000). Fracture mechanisms and instability of openings in compression. Int. J. Rock Mech. Min. Sci. 37, 263–284. https://doi.org/10.1016/S1365-1609(99)00105-7
Gitman, I.M. (2006). Representative volumes and multi-scale modelling of quasi-brittle materials. Doctoral Thesis, Delft University of Technology.
Grassl, P., Xenos, D., Nyström, U., Rempling, R., Gylltoft, K. (2013). CDPM2: A damage-plasticity approach to modelling the failure of concrete. Int. J. Solids Struct. https://doi.org/10.1016/j.ijsolstr.2013.07.008
Gribanov, I., Taylor, R., Sarracino, R. (2018). Cohesive zone micromechanical model for compressive and tensile failure of polycrystalline ice. Eng. Fract. Mech. https://doi.org/10.1016/j.engfracmech.2018.04.023
Gürtner, A. (2009). Experimental and Numerical Investigations of Ice-Structure Interaction. Doctoral Thesis. NTNU Norwegian University of Science and Technology.

Herzog, D., Seyda, V., Wycisk, E., Emmelmann, C. (2016). Acta Materialia Additive manufacturing of metals. Acta Mater. 117, 371–392. https://doi.org/10.1016/j.actamat.2016.07.019

Hillerborg, A. (1991). Application of the fictitious crack model to different types of materials. Int. J. Fract. 51, 95–102. https://doi.org/10.1007/BF00033972

Hillerborg, A., Modéer, M., Petersson, P.E. (1976). Analysis of crack formation and crack growth in concrete by means of fracture mechanics and finite elements. Cem. Concr. Res. https://doi.org/10.1016/0008-8846(76)90007-7

Hoover, C.G., Bažant, Z.P. (2014). Cohesive crack, size effect, crack band and work-of-fracture models compared to comprehensive concrete fracture tests. Int. J. Fract. https://doi.org/10.1007/s10704-013-9926-0

Horii, H., Nemat-Nasser, S. (1985). Compression-induced microcrack growth in brittle solids: Axial splitting and shear failure. J. Geophys. Res. 90, 3105. https://doi.org/10.1029/JB090iB04p03105

Horii, H., Nemat-Nasser, S. (1986). Brittle Failure in Compression: Splitting, Faulting and Brittle-Ductile Transition. Philos. Trans. R. Soc. A Math. Phys. Eng. Sci. 319, 337–374. https://doi.org/10.1098/rsta.1986.0101

Iliescu, D., Schulson, E.M. (2004). The brittle compressive failure of fresh-water columnar ice loaded biaxially. Acta Mater. https://doi.org/10.1016/j.actamat.2004.07.027

Ince, S.T., Kumar, A., Paik, J.K. (2017). A new constitutive equation on ice materials. Ships Offshore Struct. https://doi.org/10.1080/17445302.2016.1190122

Jäger, P., Steinmann, P., Kuhl, E. (2009). Towards the treatment of boundary conditions for global crack path tracking in three-dimensional brittle fracture. Comput. Mech. 45, 91–107. https://doi.org/10.1007/s00466-009-0417-0

Jordaan, I.J. (2001). Mechanics of ice-structure interaction. Eng. Fract. Mech. https://doi.org/10.1016/S0013-7944(01)00032-7

Jordaan, I.J., Matskevitch, D.G., Meglis, I.L. (1999). Disintegration of ice under fast compressive loading, in: International Journal of Fracture. https://doi.org/10.1023/a:1018605517923

Ju, J.W. (1991). On two-dimensinal self-consistent micromechanical damage models for brittle solids. Int. J. Solids Struct. 27, 227–258. https://doi.org/10.1016/0020-7683(91)90230-D

Kachanov, L.M. (1958). Time of rupture process under creep conditions. Isv. Akad. Nauk. SSR. Otd Tekh. Nauk.

Kachanov, M. (1987). Elastic solids with many cracks: A simple method of analysis. Int. J. Solids Struct. https://doi.org/10.1016/0020-7683(87)90030-8

Kachanov, M. (1993). Elastic solids with many cracks and related problems. Adv. Appl. Mech. 30, 259–445.

Kachanov, M. (2003). On the problems of crack interactions and crack coalescence. Int. J. Fract. 120, 537–543. https://doi.org/10.1023/A:1025448314409

Kachanov, M., Shafiro, B., Tsukrov, I. (2003). Handbook of Elasticity Solutions. Springer Netherlands. https://doi.org/10.1007/978-94-017-0169-3

Kolari, K. (2017). A complete three-dimensional continuum model of wing-crack growth in granular brittle solids. Int. J. Solids Struct. 115–116, 27–42. https://doi.org/10.1016/j.ijsolstr.2017.02.012

Kumar, S., Barai, S. V. (2011). Concrete fracture models and applications, Concrete Fracture Models and Applications. https://doi.org/10.1007/978-3-642-16764-5

Kurumatani, M., Terada, K., Kato, J., Kyoya, T., Kashiyama, K. (2016). An isotropic damage model based on fracture mechanics for concrete. Eng. Fract. Mech. https://doi.org/10.1016/j.engfracmech.2016.01.020

Lecampion, B., Bunger, A., Zhang, X. (2018). Numerical methods for hydraulic fracture propagation: A review of recent trends. J. Nat. Gas Sci. Eng. https://doi.org/10.1016/j.jngse.2017.10.012

Lee, J., Fenves, G.L. (1998). Plastic-damage model for cyclic loading of concrete structures. J. Eng. Mech. 124, 892–900. https://doi.org/10.1061/(ASCE)0733-9399(1998)124:8(892)

Lehner, F., Kachanov, M. (1996). On modelling of winged cracks forming under compression. Int. J. Fract. 77, 69–75.

Lemaitre, J. (1992). A Course on Damage Mechanics, A Course on Damage Mechanics.

https://doi.org/10.1007/978-3-662-02761-5
Lemaitre, J., Desmorat, R. (2005). Engineering damage mechanics: Ductile, creep, fatigue and brittle failures, Engineering Damage Mechanics: Ductile, Creep, Fatigue and Brittle Failures. https://doi.org/10.1007/b138882
Li, Q.M., Reid, S.R., Wen, H.M., Telford, A.R. (2005). Local impact effects of hard missiles on concrete targets. Int. J. Impact Eng. 32, 224–284. https://doi.org/10.1016/j.ijimpeng.2005.04.005
Li, Y.P., Chen, L.Z., Wang, Y.H. (2005). Experimental research on pre-cracked marble under compression. Int. J. Solids Struct. 42, 2505–2516. https://doi.org/10.1016/j.ijsolstr.2004.09.033
Liu, Z., Amdahl, J., Løset, S. (2011). Plasticity based material modelling of ice and its application to ship-iceberg impacts. Cold Reg. Sci. Technol. https://doi.org/10.1016/j.coldregions.2010.10.005
Lu, W., Lubbad, R., Løset, S. (2014). Simulating ice-sloping structure interactions with the cohesive element method. J. Offshore Mech. Arct. Eng. https://doi.org/10.1115/1.4026959
Määttänen, M., Marjavaara, P., Saarinen, S., Laakso, M. (2011). Ice crushing tests with variable structural flexibility. Cold Reg. Sci. Technol. 67, 120–128. https://doi.org/10.1016/j.coldregions.2011.03.004
Mazars, J., Pijaudier-Cabot, G. (1996). From damage to fracture mechanics and conversely: A combined approach. Int. J. Solids Struct. https://doi.org/10.1016/0020-7683(96)00015-7
Mohammadnejad, M., Liu, H., Chan, A., Dehkhoda, S., Fukuda, D. (2018). An overview on advances in computational fracture mechanics of rock. Geosystem Eng. 9328, 1–24. https://doi.org/10.1080/12269328.2018.1448006
Montagut, E., Kachanov, M. (1988). On modelling a microcracked zone by "weakened" elastic material and on statistical aspects of crack-microcrack interactions. Int. J. Fract. https://doi.org/10.1007/BF00032537
Mulmule, S. V., Dempsey, J.P. (1997). Stress-Separation Curves for Saline Ice Using Fictitious Crack Model. J. Eng. Mech. https://doi.org/10.1061/(asce)0733-9399(1997)123:8(870)
Murakami, Y. (1992). Stress intensity factors handbook. Pergamon Press.
Murakami, Y. (2019). Additive manufacturing: effects of defects, in: Metal Fatigue. Elsevier, pp. 453–483. https://doi.org/10.1016/B978-0-12-813876-2.00018-2
Needleman, A. (1990). An analysis of decohesion along an imperfect interface. Int. J. Fract. https://doi.org/10.1007/BF00018611
Nemat-Nasser, S., Hori, M. (Muneo) (1993). Micromechanics : overall properties of heterogeneous materials. North-Holland.
Ottosen, N., Ristinmaa, M. (2005). The Mechanics of Constitutive Modeling, The Mechanics of Constitutive Modeling. https://doi.org/10.1016/B978-0-08-044606-6.X5000-0
Paavilainen, J., Tuhkuri, J., Polojärvi, A. (2011). 2D numerical simulations of ice rubble formation process against an inclined structure. Cold Reg. Sci. Technol. https://doi.org/10.1016/j.coldregions.2011.05.003
Paliwal, B., Ramesh, K.T. (2008). An interacting micro-crack damage model for failure of brittle materials under compression. J. Mech. Phys. Solids. https://doi.org/10.1016/j.jmps.2007.06.012
Papanastasiou, P., Sarris, E. (2017). Cohesive zone models, in: Porous Rock Fracture Mechanics: With Application to Hydraulic Fracturing, Drilling and Structural Engineering. https://doi.org/10.1016/B978-0-08-100781-5.00006-3
Paterson, M.S., Wong, T.F. (2005). Experimental rock deformation - The brittle field. Springer, Berlin, Heidelberg. https://doi.org/10.1007/b137431
Pensée, V., Kondo, D., Dormieux, L. (2002). Micromechanical Analysis of Anisotropic Damage in Brittle Materials. J. Eng. Mech. https://doi.org/10.1061/(asce)0733-9399(2002)128:8(889)
Planas, J., Elices, M., Guinea, G. V., Gómez, F.J., Cendón, D.A., Arbilla, I. (2003). Generalizations and specializations of cohesive crack models. Eng. Fract. Mech. 70, 1759–1776. https://doi.org/10.1016/S0013-7944(03)00123-1
Polojärvi, A., Tuhkuri, J. (2013). On modeling cohesive ridge keel punch through tests with a combined finite-discrete element method. Cold Reg. Sci. Technol.

https://doi.org/10.1016/j.coldregions.2012.09.013
Rashid, Y.R. (1968). Ultimate strength analysis of prestressed concrete pressure vessels. Nucl. Eng. Des. https://doi.org/10.1016/0029-5493(68)90066-6
Renshaw, C.E., Schulson, E.M. (2001). Universal behaviour in compressive failure of brittle materials. Nature 412, 897–900.
Sanaei, N., Fatemi, A., Phan, N. (2019). Defect characteristics and analysis of their variability in metal L-PBF additive manufacturing. Mater. Des. https://doi.org/10.1016/j.matdes.2019.108091
Sand, B. (2008). Nonlinear finite element simulations of ice forces on offshore structures. Doctoral Thesis. Luleå University of Technology.
Santaoja, K. (2019). On continuum damage mechanics. Raken. Mek. https://doi.org/10.23998/rm.76025
Schulson, E.M., Duval, P. (2009). Creep and fracture of ice, Creep and Fracture of Ice. https://doi.org/10.1017/CBO9780511581397
Schulson, E.M., Iliescu, D., Renshaw, C.E. (1999). On the triggering of shear faults during brittle compressive failure: a new mechanism. Mater. Res. Soc. Symp. - Proc.
Shah, S.P., Swartz, S.E., Ouyang, C. (1995). Fracture mechanics of concrete : applications of fracture mechanics to concrete, rock and other quasi-brittle materials. Wiley.
Shi, J., Shen, B., Stephansson, O., Rinne, M. (2014). A three-dimensional crack growth simulator with displacement discontinuity method. Eng. Anal. Bound. Elem. https://doi.org/10.1016/j.enganabound.2014.07.002
Shojaei, A., Dahi Taleghani, A., Li, G. (2014). A continuum damage failure model for hydraulic fracturing of porous rocks. Int. J. Plast. https://doi.org/10.1016/j.ijplas.2014.03.003
Song, J.H., Wang, H., Belytschko, T. (2008). A comparative study on finite element methods for dynamic fracture. Comput. Mech. 42, 239–250. https://doi.org/10.1007/s00466-007-0210-x
Sukumar, N., Dolbow, J.E., Moës, N. (2015). Extended finite element method in computational fracture mechanics: a retrospective examination. Int. J. Fract. https://doi.org/10.1007/s10704-015-0064-8
Sun, C.-T., Jin, Z. (2011). Fracture Mechanics. Academic Press.
Tada, H., Paris, P.C., Irwin, G.R. (2000). The Stress Analysis of Cracks Handbook, Third Edition, The Stress Analysis of Cracks Handbook, Third Edition. ASME Press. https://doi.org/10.1115/1.801535
Taylor, R.S., Jordaan, I.J. (2014). Damage and fracture during contact between a spherical indenter and ice: Experimental results and finite element simulations, in: Key Engineering Materials. https://doi.org/10.4028/www.scientific.net/KEM.577-578.609
Tijssens, M.G.A., Sluys, B.L.J., Van der Giessen, E. (2000). Numerical simulation of quasi-brittle fracture using damaging cohesive surfaces. Eur. J. Mech. A/Solids 19, 761–779. https://doi.org/10.1016/S0997-7538(00)00190-X
Timco, G.W., Weeks, W.F. (2010). A review of the engineering properties of sea ice. Cold Reg. Sci. Technol. 60, 107–129. https://doi.org/10.1016/j.coldregions.2009.10.003
von Bock und Polach, R., Ehlers, S. (2013). Model scale ice - Part B: Numerical model. Cold Reg. Sci. Technol. https://doi.org/10.1016/j.coldregions.2013.06.009
Wang, E.Z., Shrive, N.G. (1995). Brittle fracture in compression: Mechanisms, models and criteria. Eng. Fract. Mech. 52, 1107–1126. https://doi.org/10.1016/0013-7944(95)00069-8
Wang, F., Zou, Z.J., Zhou, L., Ren, Y.Z., Wang, S.Q. (2018). A simulation study on the interaction between sloping marine structure and level ice based on cohesive element model. Cold Reg. Sci. Technol. https://doi.org/10.1016/j.coldregions.2018.01.022
Wang, Y., Zou, Z.J., Wang, F., Shi, C., Luo, Y., Lu, T.C. (2019). A simulation study on the ice fracture behaviors in ice-lighthouse interaction considering initial defects in ice sheet. Ocean Eng. https://doi.org/10.1016/j.oceaneng.2018.12.056

Xie, D., Biggers, S.B. (2006). Progressive crack growth analysis using interface element based on the virtual crack closure technique. Finite Elem. Anal. Des. https://doi.org/10.1016/j.finel.2006.03.007

Xu, X.P., Needleman, A. (1994). Numerical simulations of fast crack growth in brittle solids. J. Mech. Phys. Solids 42, 1397–1434. https://doi.org/10.1016/0022-5096(94)90003-5

Yao, Y., Liu, L., Keer, L.M. (2015). Pore pressure cohesive zone modeling of hydraulic fracture in quasi-brittle rocks. Mech. Mater. https://doi.org/10.1016/j.mechmat.2014.12.010

Aalto-DD 192/2020

ISBN 978-952-64-0147-8 (printed)
ISBN 978-952-64-0148-5 (pdf)
ISSN 1799-4934 (printed)
ISSN 1799-4942 (pdf)

Aalto University
School of Engineering
Department of applied mechanics
www.aalto.fi

BUSINESS + ECONOMY

ART + DESIGN + ARCHITECTURE

SCIENCE + TECHNOLOGY

CROSSOVER

DOCTORAL DISSERTATIONS